

# UC Berkeley

## UC Berkeley Previously Published Works

### Title

Recombinant Protein Stability in Cyanobacteria

### Permalink

<https://escholarship.org/uc/item/8pn8s6h9>

### Journal

ACS Synthetic Biology, 10(4)

### ISSN

2161-5063

### Authors

Zhang, Xianan  
Betterle, Nico  
Martinez, Diego Hidalgo  
[et al.](#)

### Publication Date

2021-04-16

### DOI

10.1021/acssynbio.0c00610

Peer reviewed

## Recombinant Protein Stability in Cyanobacteria

Xianan Zhang,<sup>†</sup> Nico Betterle,<sup>†</sup> Diego Hidalgo Martinez,<sup>†</sup> and Anastasios Melis\*<sup>‡</sup>Cite This: <https://dx.doi.org/10.1021/acssynbio.0c00610>

Read Online

ACCESS |



Metrics &amp; More



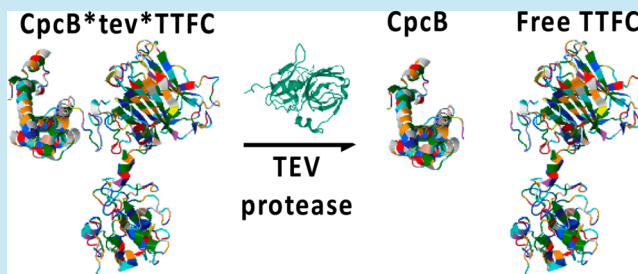
Article Recommendations



Supporting Information

**ABSTRACT:** The living cell possesses extraordinary molecular and biochemical mechanisms by which to recognize and efficiently remove foreign, damaged, or denatured proteins. This essential function has been a barrier to the overexpression of recombinant proteins in most expression systems. A notable exception is the overexpression in *E. coli* of recombinant proteins, most of which, however, end-up as “inclusion bodies”, *i.e.*, cytoplasmic aggregates of proteins that are inaccessible to the cell’s proteasome. “Fusion constructs as protein overexpression vectors” proved to be unparalleled in their ability to cause substantial accumulation of recombinant proteins from plants, animals, and bacteria, as soluble proteins in unicellular cyanobacteria. Recombinant protein levels in the range of 10–20% of the total cellular protein can be achieved. The present work investigated this unique property in the context of recombinant protein stability in *Synechocystis* sp. PCC 6803 by developing and applying an *in vivo* cellular tobacco etch virus cleavage system with the objective of separating the target heterologous proteins from their fusion leader sequences. The work provides new insights about the overexpression, cellular stability, and exploitation of transgenes with commercial interest, highly expressed in a cyanobacterial biofactory. The results support the notion that eukaryotic plant- and animal-origin recombinant proteins are unstable, when free in the cyanobacterial cytosol but stable when in a fusion configuration with a highly expressed cyanobacterial native or heterologous protein. Included in this analysis are recombinant proteins of the plant isoprenoid biosynthetic pathway (isoprene synthase,  $\beta$ -phellandrene synthase, geranyl diphosphate synthase), the human interferon protein, as well as prokaryotic proteins (tetanus toxin fragment C and the antibiotic resistance genes kanamycin and chloramphenicol). The future success of synthetic biology approaches with cyanobacteria and other systems would require overexpression of pathway enzymes to attain product volume, and the work reported in this paper sets the foundation for such recombinant pathway enzyme overexpression.

**KEYWORDS:** fusion constructs, protein overexpression, recombinant protein, *Synechocystis* sp. PCC 6803, tobacco etch virus protease



## INTRODUCTION

Phototrophic microorganisms, such as cyanobacteria and eukaryotic microalgae, have the potential to serve as platforms for large-scale production of specialty and commodity products. Several of them are already commercially exploited.<sup>1–6</sup> They are viewed as microscopic cell-factories with minimal feedstock requirements, as they only need sunlight, CO<sub>2</sub>, some low-cost mineral nutrients, and water. In addition, many microalgal species are GRAS (generally regarded as safe) microorganisms and thus are suitable for human consumption.<sup>7</sup>

Cyanobacteria drew attention in the recent past, thanks to the advancement of molecular biology and synthetic biology approaches. Indeed, the rapid and low-cost synthesis of large transgenic and codon optimized DNA constructs, coupled with the natural transformability of most cyanobacterial species, made these photosynthetic microorganisms tractable for complex genetic engineering.<sup>8–10</sup> Moreover, several cyanobacterial species have recently been reported to show growth rates that are comparable to *Saccharomyces cerevisiae*,<sup>11–13</sup> solving a

key issue arising from the otherwise relatively slow growth rate of model cyanobacteria.

Efforts were expended in recent years on the development of robust genetic tools required for the expression of heterologous proteins in cyanobacteria.<sup>14–19</sup> High-level expression of functional enzymes is imperative in the effort to increase flux and yield, if the product of interest is a specialty or commodity compound. High cellular concentration of pathway enzymes is necessary to create enough driving force in order to direct the cellular metabolism toward the synthesis of the targeted product. Certainly, high protein expression is also desirable when a biopharmaceutical protein is the product of interest.<sup>20</sup> Unfortunately, while the expression of heterologous prokaryotic proteins in cyanobacteria appears to be possible upon

Received: December 3, 2020

coupling a strong promoter and RBS to the DNA of interest,<sup>21–23</sup> the expression of eukaryotic proteins proved to be difficult, which is believed to be due to hindrances at the level of protein translation.<sup>20,24</sup>

Overexpression of eukaryotic proteins in cyanobacteria was achieved indirectly upon implementing a “fusion constructs approach”. This procedure comprised the fusion of a native or non-native gene that is highly expressed in cyanobacteria to the heterologous eukaryotic gene, with the first serving as a leader sequence.<sup>20,22,25–29</sup> It is worth noting that such an approach can be extended to include multiple transgenes fused together, as recently shown in the microalga *Chlamydomonas reinhardtii*,<sup>30</sup> encoding within a single fusion construct several enzymatic functions. However, the functionality of multi-proteins in a single fusion construct, especially when the latter entails heterologous proteins, remains to be validated. In this respect, fusion constructs can limit or even impede the catalytic activity of the participating enzymes.<sup>25</sup> Further, it is possible that the target protein cannot be used in a fusion form, as the case would be for biopharmaceutical and biotherapeutic proteins aimed for clinical use, requiring the development of technologies for a prior removal of the leader sequence.

*In vivo* cleavage of heterologous fusion proteins is desirable, when there is a need to separate the moieties of the fusion construct so as to derive the target protein in its pure form. This approach was applied in prokaryotes, such as *E. coli*<sup>31</sup> and microalgae.<sup>32</sup> In particular, *in vivo* cleavage in *E. coli* was achieved by coexpressing, along with the fusion protein of interest, the tobacco etch virus protease (TEV), with the former harboring a specific TEV cleavage site. However, TEV proved to be poorly stable in bacteria, and therefore, it required stabilization, implemented in one application by fusing the TEV to the soluble maltose binding protein (MBP), with the latter serving as the leader sequence in the construct.<sup>31</sup>

The present work developed and applied an *in vivo* TEV cleavage system in cyanobacteria that are overexpressing fusion construct proteins, with the objective of separating the target heterologous proteins from their fusion leader sequences. New insights were obtained about the overexpression, cellular stability, and potential exploitation of transgenes with commercial interest that are highly expressed in the cyanobacterial biofactory. The results are discussed in terms of differential rates of translation and stability of eukaryotic versus prokaryotic proteins in cyanobacteria.

## RESULTS

**Development and Application of the Tobacco Etch Virus Protease (TEV) Technology in Cyanobacteria.** To the best of our knowledge, overexpression of heterologous eukaryotic proteins in cyanobacteria has been achieved only through the “fusion constructs approach”.<sup>20,22,24–26</sup> Such an approach comprised a fusion of the gene encoding a target eukaryotic protein to a gene that is highly expressed in cyanobacteria. The latter could be either native to the cell or heterologous in origin. The *cpcB* gene of *Synechocystis*, encoding the abundant  $\beta$ -subunit of phycocyanin, was used as the leader fusion sequence with notable success. This approach resulted in the stable accumulation of heterologous eukaryotic proteins in cyanobacteria to hitherto unknown levels of up to 20% of the total cellular protein.<sup>20,24,28,33</sup>

The presence of a leader sequence in a fusion protein configuration is not desirable in some cases, as it can lower the

catalytic activity of the target protein<sup>25</sup> or hinder the application of the protein of interest, as the case would be for biopharmaceutical and biotherapeutic proteins aimed for clinical use,<sup>20</sup> requiring the development of technologies for a prior cleavage of the leader sequence. Work in this paper developed and applied the heterologous tobacco etch virus protease technology, hereafter referred to as TEV, in the model cyanobacteria *Synechocystis* sp. PCC 6803 (*Synechocystis*), as a process for the *in vivo* separation of leader sequences in fusion constructs after protein overexpression of the respective vectors.

Three different TEV DNA constructs were designed for the transformation and testing of wild type (WT) *Synechocystis* through double homologous DNA recombination in the *psbA2* gene locus (Figure 1A). Construct *nptI*-TEV (Figure 1B) was designed to replace the *psbA2* gene, installing the kanamycin resistance cassette (*nptI*), followed by the TEV gene in an operon configuration. The fusion construct approach was employed as an alternative method in the effort to express the

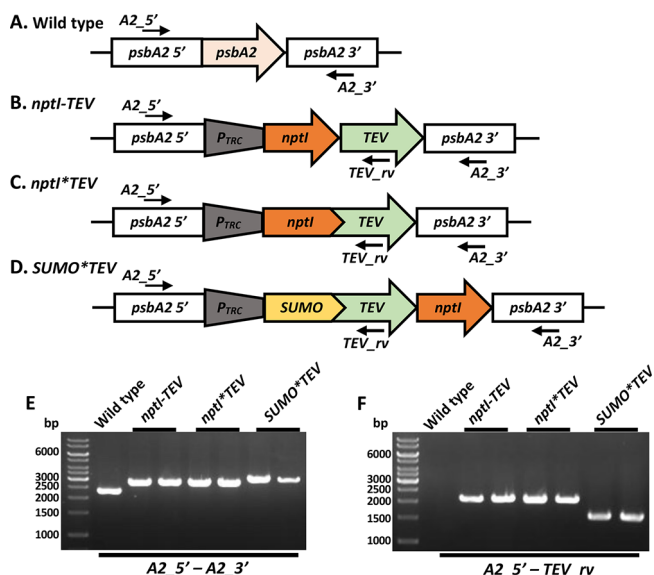


**Figure 1.** Constructs designed for expression of the TEV protease in *Synechocystis* sp. PCC 6803 (*Synechocystis*) and PCR verification of transgenic DNA homoplasmies upon transformation of *Synechocystis*. (A) The *psbA2* locus, as it occurs in wild type *Synechocystis*. This DNA sequence is referred to as the wild type (WT). Note the location of primers used in genomic DNA PCR reaction analysis, denoted by horizontal arrows. (B) Replacement of the *psbA2* gene in the *psbA2* locus with a construct comprising the  $P_{TRC}$  promoter, the kanamycin resistance cassette (*nptI*) gene, followed by the codon optimized TEV gene in an operon configuration. This DNA construct is referred to as *nptI*-TEV. (C) Replacement of the *psbA2* gene in the *psbA2* locus with a construct comprising the  $P_{TRC}$  promoter followed by the codon optimized *nptI*\*TEV genes in a fusion construct configuration with the *nptI* gene serving as a leader sequence. (D) Replacement of the *psbA2* gene in the *psbA2* locus with a construct comprising the  $P_{TRC}$  promoter followed by the codon optimized SUMO\*TEV genes in a fusion construct configuration with the SUMO gene serving as a leader sequence. (E) Genomic DNA PCR analysis testing for transgenic DNA copy homoplasmies in *Synechocystis* transformants using A2\_5' forward and A2\_3' reverse primers. Absence of WT PCR product in the transformants indicated achievement of transgenic DNA copy homoplasmies. (F) Genomic DNA PCR analysis testing for correct insertion of the transgenic DNA in *Synechocystis* transformants using A2\_5' forward and TEV\_rv reverse primers.

TEV.<sup>20,22,27</sup> In this case, the *nptI* gene itself was chosen as a leader sequence in the fusion construct, since it was shown to enhance the heterologous protein expression in cyanobacteria while, at the same time, acting as a selectable marker.<sup>27</sup> To this aim, fusion construct *nptI\*TEV* (Figure 1C) was designed to replace the *psbA2* gene in the respective locus. The SUMO gene is another known leader sequence used to enhance heterologous protein expression and stability in prokaryotic cells.<sup>34</sup> An advantage in this case is that the small size of the SUMO-encoded polypeptide (~10 kDa) limits possible steric hindrances in the fusion protein, while limiting the cost of gene synthesis. Thus, construct *SUMO\*TEV* (Figure 1D) was designed to install both the fusion construct *SUMO\*TEV* and the *nptI* gene in an operon configuration. All three constructs described above were codon optimized for expression in *Synechocystis* and designed to operate under the constitutive control of the  $P_{TRC}$  promoter. The nucleotide sequence of these constructs is given in the Supporting Information of this work.

Attainment of transgenic DNA copy homoplasmy in the three different transformant strains was tested through genomic DNA PCR analysis. Primers, *A2\_5'* forward and *A2\_3'* reverse were designed from the flanking regions of the *psbA2* DNA insertion site (Figure 1A). PCR amplification using WT genomic DNA as a template generated a product of 2,320 bp, corresponding to the *psbA2* gene (Figure 1E). PCR amplifications using DNA from two separate *nptI-TEV* and two *nptI\*TEV* transformant lines generated the anticipated product of 2,879 bp, whereas the PCR product size from two *SUMO\*TEV* transformants was 3,174 bp (Figure 1E). Attainment of DNA copy homoplasmy was evidenced by the absence of WT PCR products in the PCR reactions of the transformant lines.

Correct installation of the heterologous sequences was further tested and confirmed by conducting a genomic DNA PCR analysis with primers *A2\_5'* forward and *TEV\_rv* reverse (Figure 1D and 1F), annealing on the upstream flanking region of the insertion site (*A2\_5'*) and a DNA sequence internal to the *TEV* gene (*TEV\_rv*). With these primers, no PCR product was generated using DNA from WT *Synechocystis*, whereas the *nptI-TEV*, *nptI\*TEV*, and *SUMO\*TEV* lines generated PCR products of 2,154 bp, 2,154 bp, and 1,620 bp, respectively.

Protein analysis of total cell extracts from *Synechocystis* WT and TEV transformants was implemented through SDS-PAGE followed by Coomassie blue staining and Western blot analysis (Figure 2A and 2B). WT protein extracts showed the presence of the CpcB  $\beta$ -subunit and CpcA  $\alpha$ -subunit of phycocyanin, as the dominant cyanobacterial proteins, migrating to ~19 and ~17 kDa, respectively. Another abundant protein in the SDS-PAGE profile was the large subunit of Rubisco (RbcL), migrating to ~56 kDa (Figure 2A). The *nptI-TEV* strain failed to show a detectable presence of recombinant TEV protein (~27 kDa), suggesting that the powerful  $P_{TRC}$  promoter was not enough to support a measurable TEV protein expression or that the recombinant protein was unstable and degraded by the cell. Furthermore, no substantial accumulation of *SUMO\*TEV* (~38 kDa) and *NptI\*TEV* (~58 kDa) fusion proteins could be detected in the *SUMO\*TEV* and *nptI\*TEV* transformants, respectively. Sensitive Western blot analysis with specific polyclonal antibodies raised against the TEV protein corroborated the evidence from the Coomassie-stained SDS-PAGE. Indeed, no cross-reaction could be detected between the antibodies and any protein band in the wild type and *nptI-*

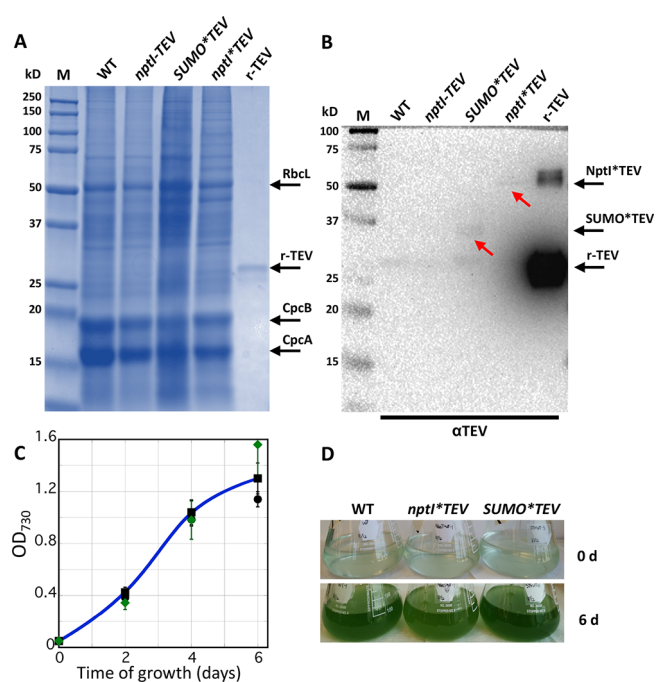


**Figure 2.** Protein expression analysis of *Synechocystis* wild type and TEV expressing transformants. (A) Total cellular protein extracts were resolved by SDS-PAGE and visualized by Coomassie-stain. Total protein extracts from wild type (WT), *nptI-TEV*, *SUMO\*TEV*, and *nptI\*TEV* transformant cells were loaded onto the SDS-PAGE. One nanogram of recombinant TEV was also loaded as a control (r-TEV). Individual native and heterologous proteins of interest are indicated to the right of the gel. Sample loading corresponds to 1  $\mu$ g of chlorophyll. (B) Total protein extracts of (A) were subjected to Western blot analysis. Specific polyclonal antibodies against the TEV were used to probe target proteins. Note the faint specific antibody cross-reaction with proteins migrating to ~38 and ~58 kDa in the *SUMO\*TEV* and *nptI\*TEV* strains, respectively, compared with the strong cross-reaction of the antibodies with the r-TEV control. (C) Biomass accumulation curves of *Synechocystis* wild type and *SUMO\*TEV* and *nptI\*TEV* transformants, as measured from the optical density of the cultures at 730 nm ( $OD_{730}$ ). Cells were grown under 100  $\mu$ mol photons  $m^{-2} s^{-1}$  of incident PAR intensity. Cultures were inoculated to an  $OD_{730}$  of about 0.05, as the initial cell concentration in the biomass accumulation experiment. Measurements were taken every 2 days through day 6 of growth with two replicates per strain. (D) Coloration of liquid cultures upon culture inoculum (0 d) and after 6 days of growth (6 d). Note that the *nptI\*TEV* and *SUMO\*TEV* transformant strains showed the same blue-green coloration as the WT.

*TEV* samples, whereas a faint cross-reaction, with the anticipated electrophoretic migration, was detected in both the *SUMO\*TEV* and *nptI\*TEV* fusion construct samples (Figure 2B, slanted red arrows). Figure 2A (r-TEV lane) also shows, as a control, the SDS-PAGE Coomassie stain of 1 ng of recombinant TEV (New England Biolabs, Ipswich, MA), whereas Figure 2B (r-TEV lane) shows the corresponding Western blot analysis. Cross-reaction intensity differences between the positive 1 ng recombinant r-TEV control and the *SUMO\*TEV* and *nptI\*TEV* protein extracts suggested a very low expression level of TEV in the latter, probably in the picogram range.

Expression of the TEV construct did not cause any cell growth impairment in the *nptI-TEV*, *nptI\*TEV*, or *SUMO\*TEV* transformants. This was evidenced by the growth curves

of these strains, which showed the same profile as the WT *Synechocystis* cultures (Figure 2C). Moreover, pigmentation of WT and transformant cultures was the same following 6 days of autotrophic growth in liquid cultures (Figure 2D), corroborating the notion that TEV expression does not negatively impact the physiology and fitness of the transformant cells.

**Recombinant Isoprene Synthase Stability in Cyanobacteria.** Despite the low-level expression of TEV in the above-mentioned *Synechocystis* transformants, the ability of the TEV enzyme in the *SUMO*\*TEV and *nptI*\*TEV lines to perform *in vivo* cleavage of heterologous fusion proteins harboring the TEV cleavage site (hereafter referred to as *tev*) was evaluated. The case study was the CpcB\*ISPS isoprene synthase fusion protein.<sup>25,33</sup> This construct, comprising the phycocyanin  $\beta$ -subunit-encoding *cpcB* gene (Figure 3A), which is naturally expressed to high levels in cyanobacteria (Figure 2A), was fused as a leader sequence to the isoprene synthase

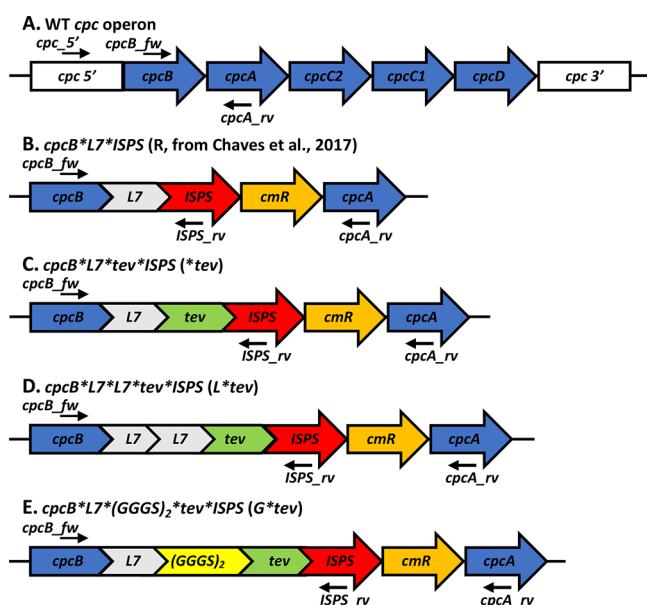


**Figure 3.** Constructs designed for the expression of CpcB\*ISPS fusion protein variants in *Synechocystis*. (A) Schematic of the *cpc* operon in the wild type. Note the location of primers used in subsequent PCR reaction analysis (Figure 4A and B), shown as horizontal forward arrows. (B) Replacement of the native *cpcB* gene with a fusion construct comprising the *cpcB*\*L7\*ISPS and the chloramphenicol resistance *cmR* cassette in the *cpc* operon locus. The phycocyanin-encoding  $\beta$ -subunit *cpcB* gene was the leader sequence in the *cpcB*\*L7\*ISPS fusion construct. The *cpcB* and ISPS genes were separated by a seven amino acid encoding L7 linker. The construct also contained the *cmR* resistance cassette in an operon configuration with the *cpcB*\*L7\*ISPS. Details about these sequences are available in ref 25. This DNA construct is referred to as the recipient *cpcB*\*L7\*ISPS. (C) Modification of *cpcB*\*L7\*ISPS fusion construct upon addition of the TEV cleavage site (*tev*) between the L7 linker and the ISPS gene, comprising the *cpcB*\*L7\*tev\*ISPS construct in the fusion configuration. This DNA construct is referred to as *\*tev*. (D) Modification of *cpcB*\*L7\*tev\*ISPS construct upon addition of a second L7 linker next to the existing L7 linker, comprising the *cpcB*\*L7\*L7\*tev\*ISPS construct in the fusion configuration. This DNA construct is referred to as the *L\*tev*. (E) Modification of *cpcB*\*L7\*ISPS fusion construct upon addition of a flexible (GGGS)<sub>2</sub> linker after the L7 linker followed by *tev* and the ISPS gene in a fusion configuration. This DNA construct is referred to as the *G\*tev*.

(ISPS) from *Pueraria montana* (kudzu). Recent work from this lab has shown that the *cpcB*\*ISPS fusion construct, thanks to its highly expressed leader sequence, stably accumulated to levels reaching 20% of the total *Synechocystis* cellular protein.<sup>25,33</sup> A functionally active *cpcB*\*ISPS fusion construct entailed insertion of a linker comprising seven amino acids (L7), designed to change the orientation of the two fusion proteins relative to one-another. The resulting *cpcB*\*L7\*ISPS fusion construct<sup>25</sup> (Figure 3B) was employed in the below-described TEV work.

The *cpcB*\*L7\*ISPS fusion construct was modified upon installation of the *tev* cleavage domain between the L7 and ISPS DNA, comprising the new *cpcB*\*L7\*tev\*ISPS fusion construct (Figure 3C). Two additional constructs, harboring different linker sequences between the *cpcB* and ISPS genes, were designed and also provided with *tev* to increase the probability of a successful cleavage by the TEV enzyme (Figure 3D and E). It is important that, prior to testing the cleavage of the desired fusion protein by TEV, the expression level of the target fusion protein itself had to be evaluated. This is because the linker domain between the two moieties of the fusion protein could affect the accumulation of the desired polypeptide, as described in previous literature.<sup>25</sup>

Transformation and attainment of transgenic DNA copy homoplasmy for the recipient *cpcB*\*L7\*ISPS (R), *cpcB*\*L7\*tev\*ISPS (*\*tev*), *cpcB*\*L7\*L7\*tev\*ISPS (*L\*tev*), and *cpcB*\*L7\*(GGGS)<sub>2</sub>\*tev\*ISPS (*G\*tev*) lines were tested and verified by genomic DNA PCR analysis using specific *cpc\_5'* forward and *cpcA\_rv* reverse primers (Figure 4A). The absence of WT PCR product in the amplification from the transformant strain templates indicated achievement of transgenic DNA copy homoplasmy. Correct installation of the recombinant constructs was tested and verified using primers *cpcB\_fw*–*ISPS\_rv*, annealing on the endogenous *cpcB* and heterologous ISPS gene sequences, respectively (Figures 3 and 4B). In this case, the wild type gave no PCR products, whereas R, *L\*tev*, *\*tev*, and *G\*tev* transformants yielded the anticipated 866 bp, 908 bp, 887 bp, and 911 bp products, respectively. Phenotypically, these transformants lost the blue-green culture coloration and became more greenish-like, underlining disruption in the proper expression of the phycocyanin *cpc* operon and the associated inability of the cells to assemble the phycobilisome peripheral rods. The absence of phycocyanin from the *cpcB*\*fusion transformants was further evidenced in the measurement of their absorbance spectra, all of which lacked the pronounced PBS absorbance band with a peak at 625 nm, which was clearly evident in the wild type (Figure S1).

The expression level of the ISPS gene was probed by Western blot analysis with specific polyclonal antibodies raised against the ISPS protein.<sup>25</sup> Strains *cpcB*\*L7\*tev\*ISPS (*\*tev*) and *cpcB*\*L7\*(GGGS)<sub>2</sub>\*tev\*ISPS (*G\*tev*) failed to accumulate the respective fusion protein at a level comparable to that of the *cpcB*\*L7\*ISPS (R) control strain (band marked as CpcB\*ISPS, Figure 4C). On the contrary, transformant strain *cpcB*\*L7\*L7\*tev\*ISPS (*L\*tev*) successfully accumulated the target fusion protein in quantities that exceeded those of the R control. Thus, the *cpcB*\*L7\*L7\*tev\*ISPS (*L\*tev*) was chosen as the strain to evaluate the *in vivo* cleavage of the fusion protein by TEV.

The *L\*tev* strain was further transformed with each of the three TEV-encoding constructs shown in Figure 1B, C, and D, respectively, for the cyanobacterial expression of TEV. Attainment of transgenic DNA copy homoplasmy in the

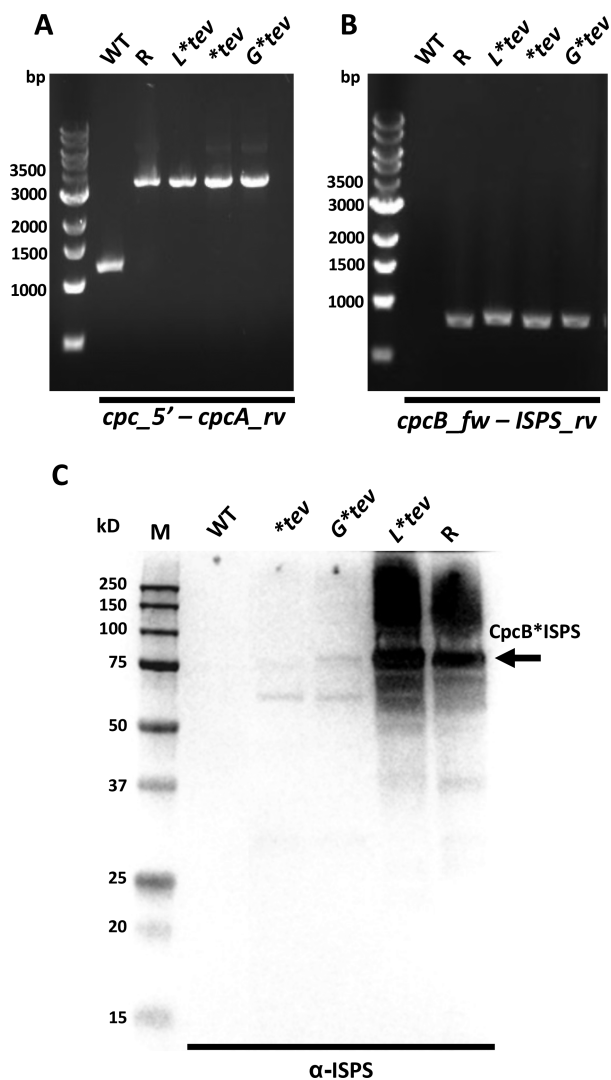


**Figure 4.** Genomic DNA and protein analyses of transformant *Synechocystis* expressing variants of the CpcB\*ISPS fusion protein. (A) Genomic DNA PCR analysis testing for transgenic DNA copy homoplasmy in *Synechocystis* transformants using *cpc\_5'* forward and *cpcA\_rv* reverse primers (Figure 3). Absence of WT PCR product in the transformants indicated achievement of transgenic DNA copy homoplasmy. (B) Genomic DNA PCR analysis testing for the correct insertion of the transgenic DNA in *Synechocystis* transformants using *cpcB\_fw* and *ISPS\_rv* primers. (C) Evaluation of the expression level of CpcB\*ISPS fusion variants in the transformants of *Synechocystis*. Analysis was conducted using rabbit-raised polyclonal antibodies against the ISPS protein, as previously described.<sup>25</sup> Sample loading corresponds to 0.5  $\mu$ g of chlorophyll. Note the strong cross-reaction of the antibodies with protein bands in the extracts from the *cpcB\*L7\*ISPS* (R) and *cpcB\*L7\*L7\*tev\*ISPS* (*L\*tev*) strains and the almost absence of a cross-reaction with extracts from the *\*tev* and *G\*tev* transformant cells.

double transformant strains *L\*tev+nptI-TEV*, *L\*tev+nptI\*TEV*, and *L\*tev+SUMO\*TEV* was tested through genomic DNA PCR analysis (Figure 5A). PCR amplification with primers *A2\_5'* forward and *A2\_3'* reverse, designed from the flanking regions of the DNA insertion site (Figure 1A), generated a product of 2,320 bp using genomic DNA as a template from WT and recipient strain *L\*tev*. PCR amplifications using DNA from the two separate *L\*tev+nptI-TEV* and two *L\*tev+nptI\*TEV* double transformant strains generated the

anticipated product of 2,879 bp, whereas the PCR product size from two *L\*tev+SUMO\*TEV* double transformants was 3,174 bp. Attainment of DNA copy homoplasmy was evidenced by the absence of WT PCR product in the PCR reactions of the transformant lines. Correct installation of the heterologous sequences was further tested by conducting a genomic DNA PCR analysis with primers *A2\_5'* forward and *TEV\_rv* reverse (Figure 5B), annealing on the upstream flanking of the insertion site (*A2\_5'*) and a DNA sequence internal to the *TEV* gene (*TEV\_rv*) (Figure 1B–D), as the reverse primer of the PCR reaction. With these primers, no PCR product was generated using DNA from WT and recipient *L\*tev* strains, whereas the *L\*tev+nptI-TEV*, *L\*tev+nptI\*TEV*, and *L\*tev+SUMO\*TEV* double transformants generated the anticipated PCR products of 2,154 bp, 2,154 bp, and 1,620 bp, respectively.

Protein analysis of total cell extracts from WT and the double transformants of *Synechocystis* was undertaken through SDS-PAGE followed by Coomassie blue staining (Figure 5C) and Western blot analysis (Figure 5D). WT protein extracts showed the presence of the CpcB  $\beta$ -subunit and CpcA  $\alpha$ -subunit of phycocyanin, as the dominant protein bands migrating to the  $\sim$ 19 and  $\sim$ 17 kDa regions. Both *L\*tev* and *L\*tev+nptI-TEV* strains showed the absence of the CpcB and CpcA subunits and substantial accumulation of the fusion CpcB\*L7\*L7\*tev\*ISPS protein, migrating to  $\sim$ 84 kDa (marked as CpcB\*ISPS, Figure 5C). On the other hand, strains *L\*tev+nptI\*TEV* and *L\*tev+SUMO\*TEV* showed much lower levels of the CpcB\*L7\*L7\*tev\*ISPS fusion, as evidenced by the faint protein bands in the respective  $\sim$ 84 kDa electrophoretic mobility region. Noteworthy in the latter was the appearance of a new protein band migrating to  $\sim$ 21 kDa in these double transformants extracts. The molecular weight corresponding to this protein band was consistent with the expected size of the CpcB cleaved subunit, resulting from the TEV cleavage of the CpcB\*L7\*L7\*tev\*ISPS fusion protein, thereby releasing the CpcB\*L7\*L7\*tev moiety. Indeed, the CpcB\*L7\*L7\*tev cleaved subunit ( $\sim$ 21 kDa) was expected to have a greater size than the native CpcB subunit ( $\sim$ 19 kDa) since the former includes the linker L7\*L7\*tev domain. The cleavage of the *tev* domain would also release the ISPS protein, possessing one additional glycine at the N-terminal domain as a result of TEV cleavage.

Identification of the protein bands discussed above was implemented by Western blot analysis (Figure 5D) using specific polyclonal antibodies raised against the CpcB protein (PhytoAB, Redwood City, CA). A cross-reaction between the polyclonal antibodies and the CpcB  $\sim$ 19 kDa subunit in WT protein extracts confirmed the ability of polyclonal antibodies to detect this target. Evidence of cross-reaction between the  $\alpha$ -CpcB antibodies and the newly emerging  $\sim$ 21 kDa protein band in the *L\*tev+nptI\*TEV* and *L\*tev+SUMO\*TEV* double transformants strengthened the notion that the  $\sim$ 21 kDa protein band is the CpcB subunit with the addition of the linker L7\*L7\*tev residue. This is shown in Figure 5D, marked by the CpcB-cl to designate the proposed TEV cleavage activity. Further support is provided by the *L\*tev* strain, which did not express TEV and which was totally devoid of the CpcB-cl fragment but showed antibody cross-reaction with the uncleaved 84 kDa fusion protein (Figure 5D). Accordingly, this Western blot analysis is consistent with the Coomassie-stained SDS-PAGE evidence that the  $\sim$ 21 kDa CpcB-cl polypeptide is clearly present in the *L\*tev+nptI\*TEV* and *L\*tev*

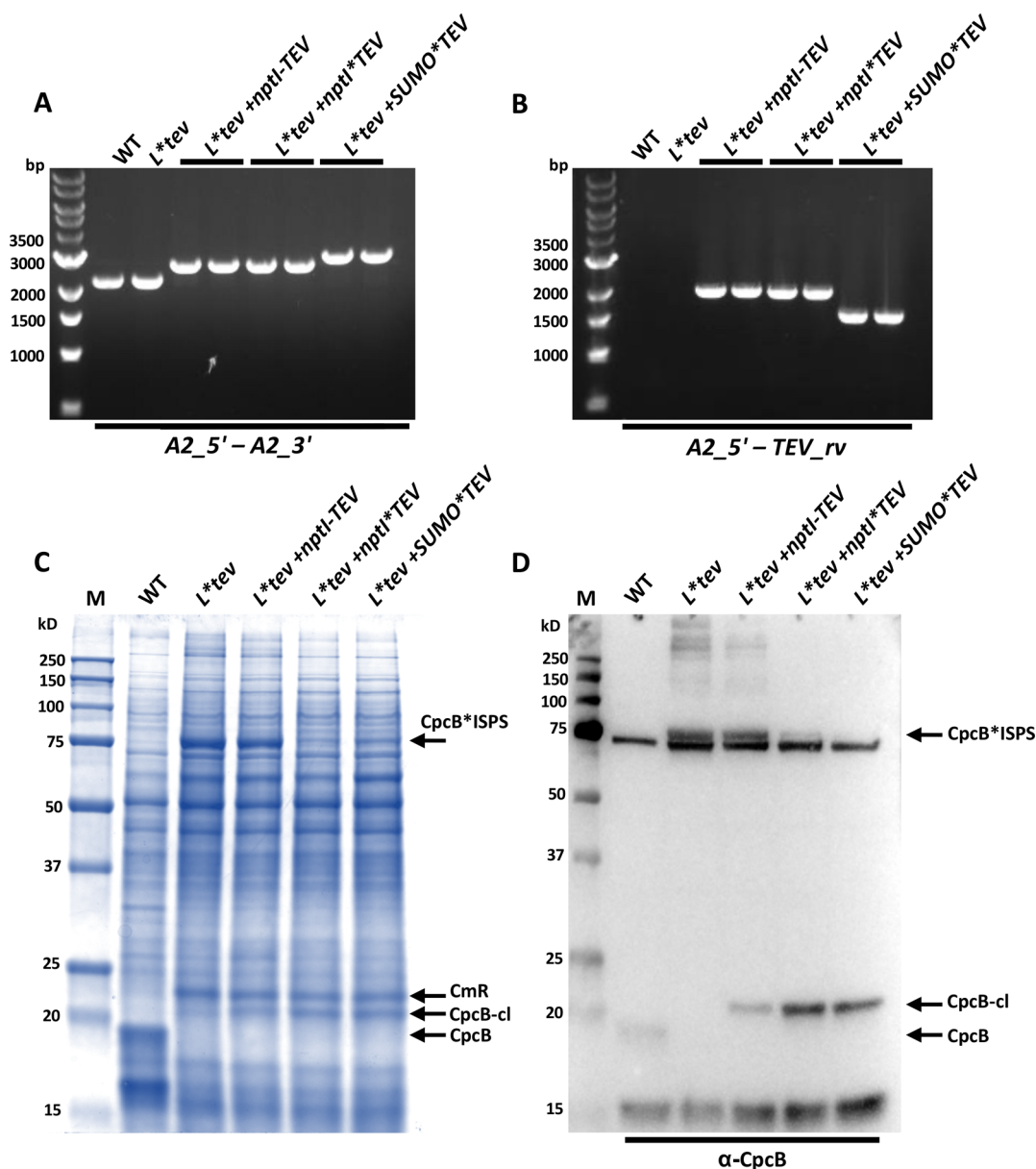


**Figure 5.** Genomic and protein analyses of double transformants expressing both CpcB\*ISPS fusion and TEV variants. (A) Genomic DNA PCR analysis testing for transgenic DNA copy homoplasmy in *Synechocystis* *cpcB*\*L7\*L7\**tev*\*ISPS (*L*\**tev*) transformants upon installation of the TEV constructs shown in Figure 1. A2\_5' forward and A2\_3' reverse primers (Figure 1) were used for the PCR reaction analysis. The absence of WT PCR product in the double transformants indicated achievement of transgenic DNA copy homoplasmy. (B) Genomic DNA PCR analysis testing for correct insertion of the transgenic DNA in *Synechocystis* transformants using A2\_5' forward and TEV\_rv reverse primers. (C) Total cellular protein extracts were resolved by SDS-PAGE and visualized by Coomassie-stain. Total protein extracts from wild type (WT), *cpcB*\*L7\*L7\**tev*\*ISPS (*L*\**tev*) transformant, and *L*\**tev*+*nptI*-TEV, *L*\**tev*+*nptI*\*TEV and *L*\**tev*+SUMO\*TEV double transformant cells were loaded onto the SDS-PAGE lanes. Individual native and heterologous proteins of interest are indicated to the right of the gel. Sample loading corresponds to 0.5  $\mu$ g of chlorophyll. Notice the accumulation of the ~84 kDa CpcB\*L7\*L7\**tev*\*ISPS fusion protein in the *L*\**tev* and *L*\**tev*+*nptI*-TEV samples, the vastly lower amounts of this ~84 kDa fusion protein in the *L*\**tev*+*nptI*\*TEV and *L*\**tev*+SUMO\*TEV double transformants, and the appearance of a ~21 kDa cleavage product (CpcB-cl) in the latter. (D) Total protein extracts of (C) were subjected to Western blot analysis. Specific polyclonal antibodies against the CpcB subunit of phycocyanin were used to probe target proteins. Note the presence of the ~21 kDa CpcB-cl protein, as indicated by the cross-reaction with CpcB antibodies, supporting the notion of a successful cleavage of the CpcB\*L7\*L7\**tev*\*ISPS fusion protein by the TEV.

+SUMO\*TEV protein extracts. The *L*\**tev*+*nptI*-TEV strain extract also showed traces of the ~21 kDa CpcB-cl but the majority of the CpcB\*L7\*L7\**tev*\*ISPS fusion remained as an uncleaved ~84 kDa protein (Figures 5C and 5D). The reason for the latter is probably due to the very low TEV expression level in the transformant harboring the *nptI*-TEV construct (Figure 2B).

The above results suggest that TEV activity in cyanobacteria is positively correlated with the TEV gene expression level. However, whereas the CpcB-cl protein was readily detected in both the Coomassie-stained SDS-PAGE and Western blot, the ISPS moiety from the TEV cleavage of the corresponding fusion construct (a putative ~63 kDa protein, hereafter referred to as ISPS-cl) could not be detected. To investigate

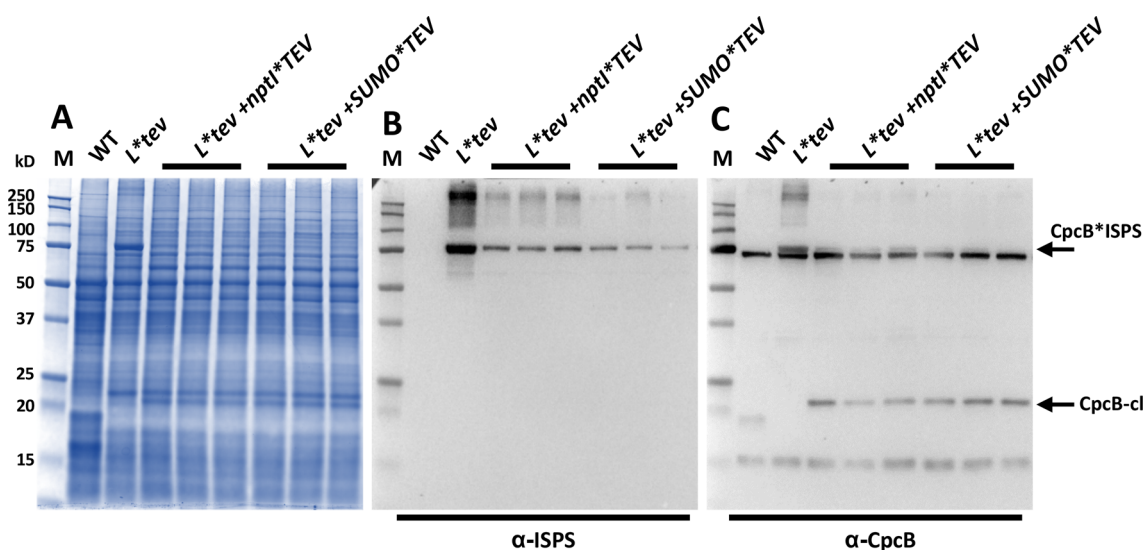


**Figure 6.** Comparison of the accumulation of cleaved ISPS (ISPS-cl) and cleaved CpcB (CpcB-cl) moieties in the  $L^{*tev+nptI*TEV}$  and  $L^{*tev+SUMO*TEV}$  double transformants. (A) Total cellular protein extracts were resolved by SDS-PAGE and visualized by Coomassie-stain. Extracts from wild type (WT),  $cpcB*L7*L7^{*tev}*ISPS$  ( $L^{*tev}$ ), and three replicates of the  $L^{*tev+nptI*TEV}$  and  $L^{*tev+SUMO*TEV}$  double transformants were loaded onto the SDS-PAGE lanes. Sample loading corresponds to 0.5  $\mu$ g of chlorophyll. Individual native and heterologous proteins of interest are indicated to the right of the gel. (B) Total protein extracts of (A) were subjected to Western blot analysis with specific polyclonal antibodies raised against the ISPS protein. Note the strong antibody cross-reaction with a protein band migrating to  $\sim$ 84 kDa in the  $L^{*tev}$  lane and the weaker cross-reactions with bands of  $\sim$ 84 kDa in the double transformants. Also note the absence of a putative ISPS-cl in the anticipated  $\sim$ 63 kDa region. (C) Total protein extracts of (A) were subjected to Western blot analysis with polyclonal antibodies against the CpcB subunit of phycocyanin. Note the antibody cross-reaction with a protein band migrating to  $\sim$ 84 kDa in the  $L^{*tev}$  lane and the much weaker cross-reaction with bands of  $\sim$ 84 kDa in the double transformants. Also note the presence of the CpcB-cl in the anticipated  $\sim$ 21 kDa region.

the fate of the anticipated ISPS-cl polypeptide, three independent biological replicates of both the  $L^{*tev+nptI*TEV}$  and  $L^{*tev+SUMO*TEV}$  double transformants were assayed by Coomassie-stained SDS-PAGE and Western blot analyses with polyclonal antibodies specific for the ISPS or CpcB polypeptides (Figure 6). The Coomassie-stained SDS-PAGE showed the presence of the abundant  $\sim$ 84 kDa CpcB\*ISPS fusion protein in the  $L^{*tev}$  strain, as expected (Figure 6, left panel). The abundance of this fusion protein was lowered in all the double transformants, when compared to the  $L^{*tev}$  strain, consistent with the notion of a successful TEV-mediated cleavage of the fusion protein. The same pattern was observed upon probing the protein profile of Figure 6 (left panel) with specific polyclonal antibodies raised against the ISPS protein (Figure 6, middle panel). It is important that a TEV-induced lowering of the CpcB\*ISPS abundance in the double transformants, as a result of TEV activity, was not balanced with the appearance of a protein band at  $\sim$ 63 kDa that could be attributed to conversion and accumulation of the free ISPS-cl. This result suggested that ISPS-cl, upon cleavage from the CpcB\*L7\*L7\*tev\*ISPS fusion protein, is unstable and is readily degraded by the cyanobacteria cells. This hypothesis was corroborated by the fact that, contrary to ISPS-cl, the CpcB-cl moiety accumulated in the  $L^{*tev+nptI*TEV}$  and  $L^{*tev+SUMO*TEV}$  double transformants, shown by both the SDS-PAGE Coomassie stained results (Figure 6, left panel) and Western blot analysis with antibodies raised against the CpcB protein (Figure 6, right panel), as already demonstrated in the results of Figure 5C and 5D.

The degradation of cleaved ISPS-cl was investigated in different growth stages of the transformant cultures. In this effort, high cell-density cultures of WT,  $L^{*tev}$ ,  $L^{*tev+nptI*TEV}$ , and  $L^{*tev+SUMO*TEV}$  strains were diluted to  $OD_{730}$  0.05 and then grown autotrophically. Cells were

harvested every 2 days through 6 days of growth. It was of interest to observe differences in pigmentation between these cell cultures (Figure 7A). Indeed, after 6 days of growth, WT cells showed the typical blue-green coloration defined by the dominant presence of phycocyanin and chlorophyll in cyanobacteria (Figure 7A, WT), whereas the  $L^{*tev}$  transformants showed a faint bluish and mostly green coloration (Figure 7A,  $L^{*tev}$ ), suggesting phycocyanin deficiency and disruption of the phycobilisome light harvesting antenna. By comparison, the double transformants showed an as yet greener pigmentation (Figure 7A,  $L^{*tev+nptI*TEV}$  and  $L^{*tev+SUMO*TEV}$ ). Protein extracts from harvested cells were analyzed by SDS-PAGE and by Coomassie stain (Figure 7B) and by Western blot analysis (Figure 7C) using antibodies specific for the ISPS protein. Wild type samples did not show the presence of the CpcB\*L7\*L7\*tev\*ISPS ( $L^{*tev}$ ) protein ( $\sim$ 84 kDa). On the contrary, all  $L^{*tev}$  cell extracts showed accumulation of the fusion protein CpcB\*ISPS in the Coomassie stained SDS-PAGE and further confirmed by Western blot analysis a cross-reaction of the anti-ISPS antibodies with an  $\sim$ 84 kDa band and with some higher molecular mass aggregates. It was also of interest that both  $L^{*tev+nptI*TEV}$  and  $L^{*tev+SUMO*TEV}$  double transformants showed a pattern of both accumulation of the CpcB\*L7\*L7\*tev\*ISPS fusion protein and cleavage of the latter (ISPS-cl), as evidenced by the presence of a faint ISPS band, migrating to about  $\sim$ 63 kDa (Figure 7C, right panel, shown by slanted red arrows). The pattern showed that the amount of the CpcB\*L7\*L7\*tev\*ISPS  $\sim$ 84 kDa protein was more pronounced on “day 2” and “day 4” of growth in the double transformants, although it was less than that of the  $L^{*tev}$  transformant. The double transformant samples were nearly devoid of the  $\sim$ 84 kDa fusion construct on “day 6” of growth. Accordingly, this analysis also showed a faint cross-

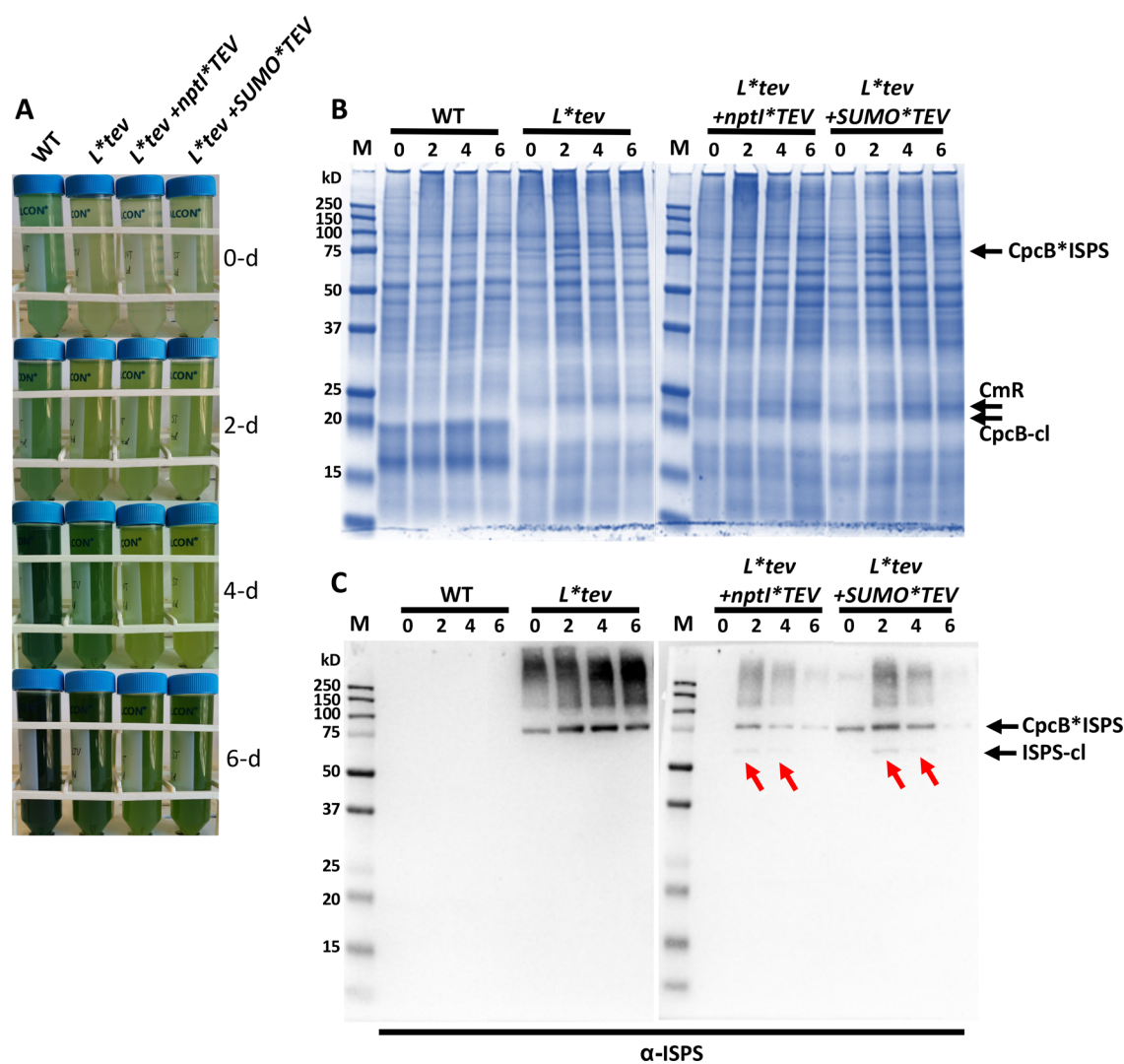


**Figure 7.** Assessment of the presence/accumulation of the ISPS-cl as a function of time during the growth of *Synechocystis* in batch cultures. (A) Cultures were inoculated at  $OD_{730} = 0.05$  and photoautotrophically grown for 6 days. A 50 mL sample from each culture was harvested every 2 days and displayed for comparative appearance. (B) Total cellular protein extracts were resolved by SDS-PAGE and visualized by Coomassie-stain. Total protein extracts from WT and the *cpcB*\*L7\*L7\**tev*\*ISPS (*L*\**tev*) transformant (Figure 7B, left panel), as well as the *L*\**tev*+*nptI*\*TEV and *L*\**tev*+SUMO\*TEV double transformants, were loaded onto the SDS-PAGE lanes, as indicated. Sample loading corresponds to 0.5  $\mu$ g of chlorophyll. Individual native and heterologous proteins of interest are marked to the right of the gel. (C) Total protein extracts of (B) were subjected to Western blot analysis with specific polyclonal antibodies raised against the ISPS protein. Note the faint presence of the ISPS-cl in the early stages of growth in the cultures (2 and 4 days of cultivation) and the absence at longer times (e.g., 6 days).

reaction between the antibodies and ISPS-cl, in the double transformants, but only in samples harvested on day 2 and day 4, referring to the early exponential growth phase of these cultures. ISPS-cl could no longer be discerned after 6 days of growth in both double transformants. These results give credence to the hypothesis that the CpcB\*L7\*L7\**tev*\*ISPS fusion confers stability to the recombinant ISPS protein. However, the free ISPS protein, emanating either as a direct expression or as a cleaved protein from a CpcB\*ISPS fusion is inherently unstable in cyanobacteria cells and subject to degradation. This instability apparently does not apply to CpcB-cl, the upstream moiety of the CpcB\*L7\*L7\**tev*\*ISPS fusion protein that is released upon TEV action, evidenced by the fact that the CpcB-cl was detected in the Coomassie stained SDS-PAGE analysis of the double transformants at all times (0 to 6 d) of culture sampling (Figures 6 and 7B, right panels, CpcB-cl).

Measurements of isoprene production in the *L*\**tev*, *L*\**tev*+*nptI*-TEV, *L*\**tev*+*nptI*\*TEV, and *L*\**tev*+SUMO\*TEV transformants were conducted, as recently described.<sup>25</sup> Isoprene accumulated in the headspace of the reactors and was sampled upon 48 and 96 h of photoautotrophic growth of cyanobacterial transformants. The overall productivity of the cyanobacterial cells (mg isoprene:g biomass) was considerably greater in the *L*\**tev* and *L*\**tev*+*nptI*-TEV strains, compared to the *L*\**tev*+*nptI*\*TEV and *L*\**tev*+SUMO\*TEV lines, after both 48 and 96 h of incubation (Figure S2). Indeed, the *L*\**tev* transformant showed the best productivity of isoprene ( $\sim 4$  mg/g), followed by the *L*\**tev*+*nptI*-TEV transformant ( $\sim 3.3$  mg/g). It was noted that *L*\**tev*+*nptI*\*TEV and *L*\**tev*+SUMO\*TEV transformants showed the lowest productivity upon 96 h of growth ( $\sim 2.4$  mg/g). All of the above suggested that stability of the ISPS as a fusion protein, and its consequential accumulation (Figure 7) played a role in sustaining isoprene production.

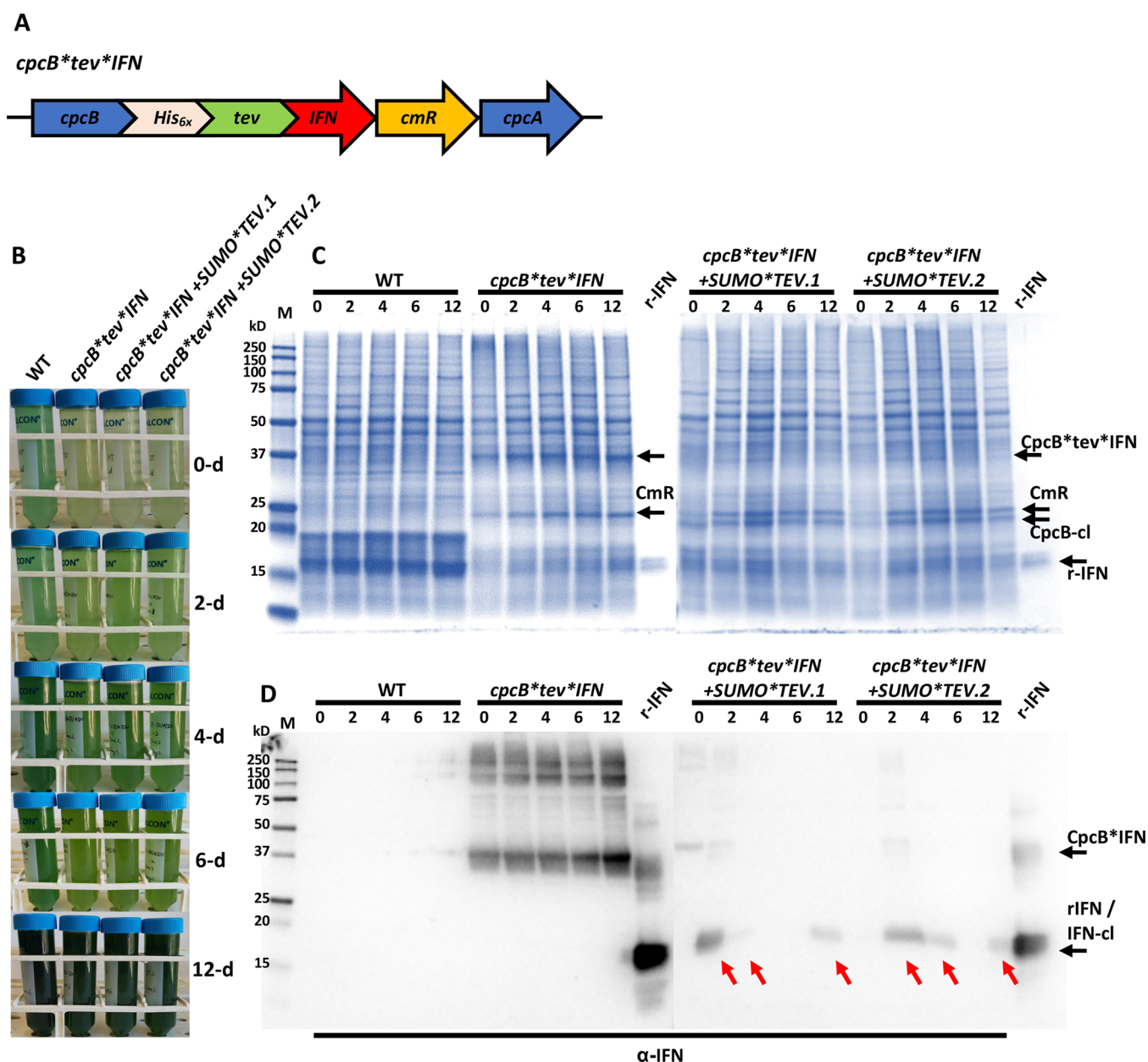


**Figure 8.** Assessment of the presence/accumulation of cleaved  $\alpha$ -interferon (IFN-cl) as a function of time during the growth of transformant *Synechocystis* in batch cultures. (A) Schematic of the *cpcB\*tev\*IFN* construct for expressing the codon-optimized human  $\alpha$ -interferon (IFN) gene as a fusion construct with the phycocyanin-encoding  $\beta$ -subunit *cpcB* gene, with the latter in the leader sequence position. The construct was adapted from previous work<sup>20</sup> replacing the factor Xa cleavage site with the TEV cleavage site (*tev*). (B) Cultures were inoculated at  $OD_{730} = 0.05$  and photoautotrophically grown for 12-days. A 50 mL sample from each culture was harvested every 2 days through day 6 and eventually after 12 days of growth, displayed here for comparative appearance. (C) Total cellular protein extracts from WT, *cpcB\*tev\*IFN* (Figure 8C, left panel), and two biological replicates of *cpcB\*tev\*IFN+SUMO\*TEV* double transformants (Figure 8C, right panel) were resolved by SDS-PAGE and visualized by Coomassie-stain. Sample loading corresponds to 0.5  $\mu$ g of chlorophyll. Individual native and heterologous proteins of interest are indicated to the right of the gel. One nanogram of recombinant IFN was also loaded as a control (r-IFN). (D) Total protein extracts of (C) were subjected to Western blot analysis with specific polyclonal antibodies raised against the IFN protein. Note the faint presence of the IFN-cl in the early stages of growth in the cultures (0–4 days of cultivation) and the declining or absent IFN-cl at longer times (e.g., 6–12 days).

This was also corroborated by the evidence that the double transformants, which did not substantially accumulate ISPS-cl, showed the lowest isoprene productivity.

#### Recombinant $\alpha$ -Interferon Stability in Cyanobacteria.

In an effort to develop a better understanding on the stability of recombinant proteins in cyanobacteria, expression of the human  $\alpha$ -interferon (IFN) was selected for testing. Recent work from this lab showed that IFN, as a CpcB\*IFN fusion construct, could accumulate in transformant cyanobacteria to

about 12% of the total cellular protein.<sup>20</sup> However, it was not clear whether cleaved IFN from a CpcB\*IFN fusion construct could be stable in the cyanobacterial cytosol. To address this question, the *cpcB\*IFN* construct<sup>20</sup> was modified to install the cleavage *tev* sequence immediately prior to the IFN-encoding DNA (Figure 8A).

The resulting recombinant strain, hereafter referred to as *cpcB\*tev\*IFN*, was then transformed again using the *SUMO\*TEV* construct (Figure 1D). Upon achievement of

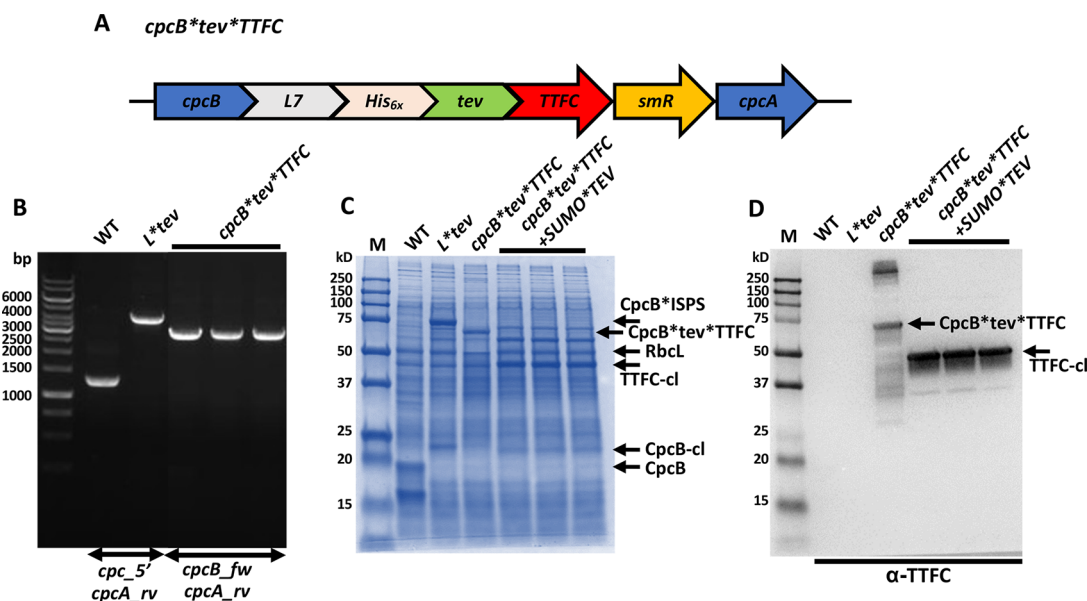


**Figure 9.** Assessment of the presence/accumulation of cleaved tetanus toxin fragment C (TTFC-cl) as a function of time during the growth of transformant *Synechocystis* in batch cultures. (A) Schematic of the DNA construct for expressing the codon-optimized tetanus toxin fragment C (TTFC) gene, as a fusion with the phycocyanin-encoding  $\beta$ -subunit *cpcB* gene, with the latter in the leader sequence position. The *cpcB\*tev\*TTFC* construct was followed by a spectinomycin resistance cassette (*smR*) in an operon configuration. The *L7* comprises DNA encoding seven amino acids, as in Figure 3, whereas *His<sub>6x</sub>* and *tev* encode the 6xHisTag and TEV cleavage sites, respectively. This construct is referred to as the *cpcB\*tev\*TTFC*. (B) Genomic DNA PCR analysis of the WT, *cpcB\*L7\*L7\*tev\*ISPS* (*L\*tev*), and the *cpcB\*tev\*TTFC* strains testing for transgenic DNA copy homoplasmy in *Synechocystis* transformants. *cpc\_5'* forward and *cpcA\_rv* reverse primers were used for the PCR analysis of WT and the *L\*tev* strains (Figure 3), whereas the *cpcB\_fw* forward and *cpcA\_rv* reverse primers were used to analyze the three *cpcB\*tev\*TTFC* lines. The absence of *L\*tev* PCR product in the transformant lines indicated achievement of transgenic DNA copy homoplasmy. (C) Total cellular protein extracts from wild type (WT), *cpcB\*L7\*L7\*tev\*ISPS* (*L\*tev*), and the *cpcB\*tev\*TTFC* transformants, as well as three replicates of the *cpcB\*tev\*TTFC+SUMO\*TEV* double transformants cells, were resolved by SDS-PAGE and visualized by Coomassie-stain. Sample loading corresponds to 0.5  $\mu$ g of chlorophyll. Individual native and heterologous proteins of interest are indicated to the right of the gel. (D) Total protein extracts of (C) were subjected to Western blot analysis with specific polyclonal antibodies raised against the TTFC protein. Note the accumulation of the CpcB\*tev\*TTFC fusion protein as a 73 kDa band in the *cpcB\*tev\*TTFC* extracts and the substantial presence of the cleaved TTFC-cl protein, migrating to  $\sim$ 52 kDa, apparently the result of a TEV cleavage of the CpcB\*tev\*TTFC fusion protein in the double transformants.

transgenic DNA copy homoplasmy, two independent replicates of the double transformant, hereafter referred to as *cpcB\*tev\*IFN+SUMO\*TEV*, were cultivated in parallel with the WT and *cpcB\*tev\*IFN* cultures (Figure 8B) in order to evaluate the cell physiology and recombinant protein stability upon TEV expression and function, following the protocol described in the results of Figure 7. Coomassie-stained SDS-PAGE showed strong accumulation of the  $\sim$ 38 kDa *cpcB\*tev\*IFN* fusion protein (Figure 8C, left panel, *cpcB\*tev\*IFN*). Consistent with the SDS-PAGE results, Western blot analysis showed that accumulation of the CpcB\*tev\*IFN recombinant protein was greater in the protein extract from the “12 days” growth than that from the other time samples (Figure 8D, left panel, *cpcB\*tev\*IFN*). Such greater accumulation in dense cultures was likely the result of enhanced *cpc* promoter activity in response to the lower average irradiance seen by the cells in high cell-density cultures. Of interest was the observation that this fusion protein was nearly absent from the two double transformants, suggesting high TEV cleavage activity (Figure 8C and D right panels). Moreover, traces of the cleaved IFN (IFN-cl) were detected via Western blot analysis only during the early cell growth exponential phase (day 2 and day 4 of growth), as previously observed with ISPS-cl (Figure 7C). Indeed, IFN-cl was not detected after “6 days of growth” in either of the double transformants (Figure 8D, right panel, slanted red arrows). A 1-ng sample of recombinant IFN (Figure 7C and D, r-IFN) was used as the control (Novus

Biologicals, Centennial, CO). These results suggested a low stability of the recombinant cleaved IFN-cl product, as observed with the ISPS-cl above.

The above results exemplify the fact that eukaryotic proteins ISPS and IFN are not well-expressed, and/or are unstable in cyanobacteria, and also provide evidence that this difficulty can be overcome by the fusion constructs approach.

**Recombinant Tetanus Toxin Fragment C (TTFC) Stability in Cyanobacteria.** ISPS and IFN are two very different proteins in terms of structure and function, deriving from a eukaryotic plant and animal system, respectively. Thus, we decided to evaluate the cyanobacterial stability, in fusion and free form, of a third protein, the prokaryotic-origin tetanus toxin fragment C (TTFC), which is noted as a candidate for a vaccine against the tetanus disease.<sup>35</sup> Construct *cpcB\*tev\*TTFC* was designed for expression of the *cpcB* and *TTFC* genes as a fusion construct, along with the spectinomycin resistance cassette (*smR*), in a modified *cpc* operon from the *L\*tev* construct (Figure 9A).

Upon transformation of the *Synechocystis L\*tev* cells, transgenic DNA copy homoplasmy was tested by genomic DNA PCR reaction analysis using specific primers *cpc\_5'* forward and *cpcA\_rv* reverse for the WT and *L\*tev* strain, or *cpcB\_fw* and *cpcA\_rv* reverse for the *cpcB\*tev\*TTFC* transformants (Figure 3A). This set of PCR reactions generated products of 1,289 bp and 3,840 bp using genomic DNA from WT and recipient *L\*tev* strain, respectively (Figure 9B).

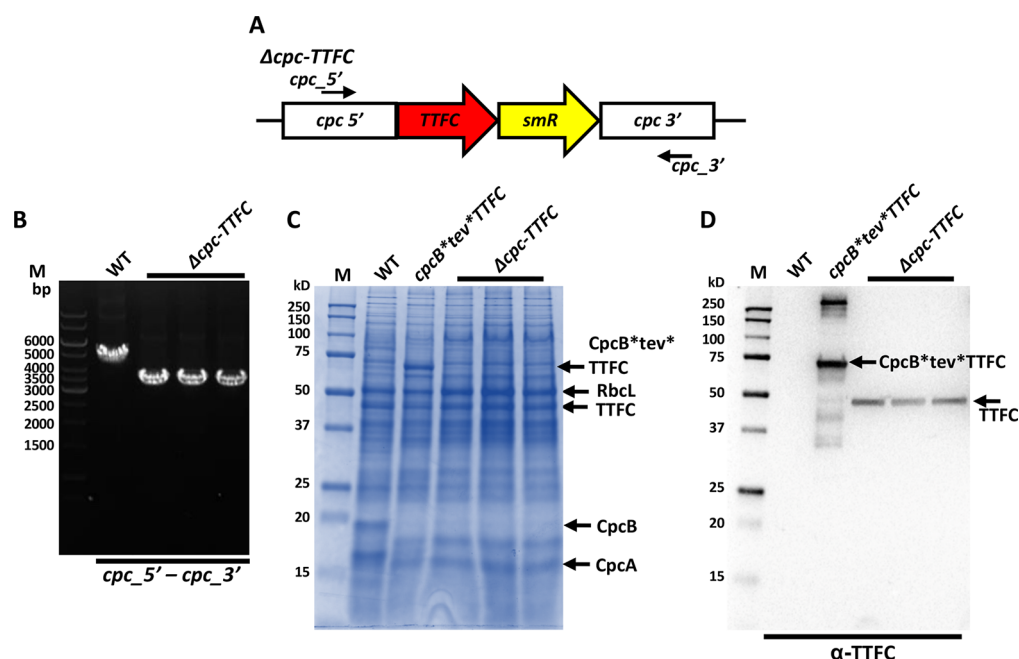


**Figure 10.** Expression of the TTFC protein directly under the control of the strong *cpc* operon promoter without employment of the fusion constructs approach. (A) Schematic of the DNA construct for expression of the codon-optimized tetanus toxin fragment C (TTFC) gene in *Synechocystis* transformants. The TTFC DNA sequence was followed by a spectinomycin resistance cassette (*smR*) in an operon configuration. This construct is referred to as the  $\Delta cpc$ -TTFC. (B) Genomic DNA PCR analysis testing for transgenic DNA copy homoplasmy in *Synechocystis* transformants using *cpc\_5'* forward and *cpc\_3'* reverse primers. The WT strain served as the recipient for the  $\Delta cpc$ -TTFC transformation. The absence of WT PCR product in the  $\Delta cpc$ -TTFC transformants indicated achievement of transgenic DNA copy homoplasmy. (C) Total cellular protein extracts from wild type (WT), *cpcB\*tev\*TTFC*, and three replicates of the  $\Delta cpc$ -TTFC transformants were loaded onto the SDS-PAGE lanes. Sample loading corresponds to 0.4  $\mu$ g of chlorophyll. Individual native and heterologous proteins of interest are indicated to the right of the gel. (D) Total protein extracts of (C) were subjected to Western blot analysis with specific polyclonal antibodies raised against the TTFC protein. Note the substantial accumulation of the ~73 kDa CpcB\*tev\*TTFC protein and the considerably lower level of the free TTFC protein from the  $\Delta cpc$ -TTFC transformants.

Whereas PCR amplifications using DNA from three replicates of *cpcB\*tev\*TTFC* transformants generated the anticipated product of 2,698 bp. The absence of WT or *L\*tev* PCR product in the *cpcB\*tev\*TTFC* transformants indicated transgenic DNA copy homoplasmy in the latter.

The *cpcB\*tev\*TTFC* strain was then transformed again with the *SUMO\*TEV* construct in the *psbA2* gene locus (Figure 1D), conferring expression of TEV. Upon transgenic DNA copy homoplasmy, tested and verified as previously shown in Figure 1E and F (results not shown), three independent replicates of the double transformant, hereafter referred to as *cpcB\*tev\*TTFC+SUMO\*TEV*, were cultivated in parallel with WT, *L\*tev*, and *cpcB\*tev\*TTFC* cultures. Coomassie-stained SDS-PAGE (Figure 9C) showed strong accumulation of the CpcB\*ISPS fusion protein (~84 kDa) in the *L\*tev* recipient strain, as already shown above in Figure 5. TTFC accumulated as a CpcB\*tev\*TTFC fusion protein, migrating to about 73 kDa. Densitometric analysis of Coomassie-stained gels, aiming to determine the percent accumulation of target protein over the total protein in the SDS-lanes, showed that CpcB\*L7\*tev\*ISPS and CpcB\*tev\*TTFC fusion proteins accumulated to 17% and 13% of total lane protein, respectively. Evidence of successful TEV cleavage activity in all three replicates of the *cpcB\*tev\*TTFC+SUMO\*TEV* double transformants was given by the accumulation of cleaved CpcB (21 kDa CpcB-cl moiety in Figure 9C) and by the presence in all *cpcB\*tev\*TTFC+SUMO\*TEV* double transformants of an abundant protein band migrating to ~52 kDa, attributed to the cleaved TTFC polypeptide (52 kDa TTFC-cl moiety in Figure 9C).

Confirmation of the identity of the latter was provided by Western blot analysis using specific polyclonal antibodies against TTFC (Antibodies-Online, Limerick, PA, United States). These results showed that TTFC-cl, emanating upon cleavage of the CpcB\*tev\*TTFC fusion protein, accumulated in the cultures to amounts that seemed to be substantially greater than that of the uncleaved fusion, suggesting a far greater stability of TTFC-cl in the cells than that shown by the ISPS-cl and IFN-cl polypeptides.

Accumulation of the bacterial TTFC-cl and the apparent stability of this cleaved protein in cyanobacteria, as opposed to that of the ISPS-cl and IFN-cl, raised the question of whether TTFC could be substantially expressed by itself (no fusion approach needed) under the control of a strong promoter. To address this question, we compared the TTFC expression level with and without employment of the fusion constructs approach, under the control of the same strong cyanobacterial *cpc* promoter. The  $\Delta cpc$ -TTFC construct (Figure 10A) was designed to express the TTFC gene, along with a spectinomycin resistance cassette (*smR*), replacing all endogenous genes in the *cpc* operon. Upon transformation of WT cells through double homologous recombination, transgenic DNA copy homoplasmy was verified by genomic DNA PCR reaction analysis using primers *cpc\_5'* forward and *cpc\_3'* reverse, designed from the flanking regions of the DNA insertion site (Figure 10A). The PCR reaction using DNA from the WT strain generated a product of 4,683 bp. Three independent biological replicates of the  $\Delta cpc$ -TTFC transformant generated the anticipated PCR products of 3,476 bp

only (Figure 10B). The absence of wild type PCR products indicated achievement of transgenic DNA copy homoplasmy. Subsequently, three independent replicates of the  $\Delta cpc$ -TTFC transformants were cultivated in parallel with the WT and  $cpcB^*tev^*TTFC$  cultures. Coomassie-stained SDS-PAGE (Figure 10C) showed strong accumulation of the  $CpcB^*tev^*TTFC$  (~73 kDa) in the  $cpcB^*tev^*TTFC$  strain. No evidence for the accumulation of the pure TTFC (~52 kDa) could be detected in the  $\Delta cpc$ -TTFC samples, although visualization of the pure TTFC protein was difficult because of the presence of native proteins in the same MW region. However, Western blot analysis with specific antibodies against TTFC (Figure 10D) clarified the picture by showing that accumulation of free TTFC from the  $\Delta cpc$ -TTFC samples was lower than that from the  $cpcB^*tev^*TTFC$  sample. This evidence corroborated the importance of the fusion constructs approach for the accumulation of the TTFC polypeptide in *Synechocystis* transformants.

It is noteworthy that the combination of the *in vivo*  $cpcB^*tev^*TTFC$ + $SUMO^*TEV$  fusion construct and cleavage product approach resulted in a substantially greater accumulation of TTFC than what was observed in the case of the  $cpcB^*tev^*TTFC$  fusion alone (Figure 9D). The visual evidence was corroborated by densitometric measurements of the Western blot analysis, where proteins were probed with antibodies against the TTFC (Table S2). This approach showed two main bands attributed to the TTFC protein (Figure 9D and 10D). A main band of ~73 kDa was attributed to the  $CpcB^*tev^*TTFC$  protein, whereas the second band of ~250 kDa was attributed to a putative aggregate containing the  $CpcB^*tev^*TTFC$ . The origin of such an aggregate can be explained since optimized solubilization procedures appeared to always leave some fusion aggregates migrating to a higher molecular weight in the gel. Cleaved TTFC accumulation in the  $cpcB^*tev^*TTFC$ + $SUMO^*TEV$  double transformant was 2.4-fold greater than that of the ~73 kDa band in the  $cpcB^*tev^*TTFC$  fusion sample. The sum of the two bands (~73 and 250 kDa) detected in the  $cpcB^*tev^*TTFC$  sample was quantitatively similar to the TTFC accumulation in the  $cpcB^*tev^*TTFC$ + $SUMO^*TEV$  sample (Table S2). This result suggested that, upon TEV cleavage, TTFC-cl accumulated in the cyanobacterial cells thanks to its high inherent stability. By comparison, TTFC accumulated poorly in the  $\Delta cpc$ -TTFC samples, i.e., to less than 40% as compared to the  $cpcB^*tev^*TTFC$  transformant. The integration of the densitometric analyses of Coomassie-stained SDS-PAGE (Figure 9C) and Western blot using  $\alpha$ -TTFC antibodies (Figure 9D) defined the accumulation of TTFC-cl in the  $cpcB^*tev^*TTFC$ + $SUMO^*TEV$  sample. As a result, TTFC-cl was found to accumulate to more than 15% of the total cell protein.

On the basis of the above-described results (Figures 9 and 10), the application of the fusion constructs approach combined with an *in vivo* cleavage appears to be the most effective method to successfully accumulate the heterologous prokaryotic TTFC protein in cyanobacteria.

## DISCUSSION

Earlier work from this and other laboratories has shown that eukaryotic plant and animal genes do not express well, at the protein level, in cyanobacteria and other photosynthetic microorganisms. This was the case of recombinant proteins encoding genes of the isoprenoid biosynthetic pathway,<sup>36–38</sup> as well as a variety of biopharmaceutical proteins.<sup>20,32,39,40</sup> The

slow or impeded rate of translation of eukaryotic recombinant proteins in cyanobacteria and possibly the chloroplast of microalgae was discussed as one of the reasons for the low yield.<sup>24</sup> This is typically manifested as a relatively high-density polyribosomes (ribosome-binding mRNAs), implicating a long ribosome dwell time on the respective mRNA.<sup>41</sup> The slow ribosome movement progression on the mRNA is causing a pile-up during translation, resulting in a slower rate of synthesis and relatively low levels of accumulation of such recombinant proteins.

A different hindrance is the possible toxicity of recombinant proteins to the prokaryotic cell. An example is offered by the work of Desplancq et al.,<sup>42</sup> who showed that eukaryotic (human) oncogene proteins, when transgenically expressed in cyanobacteria, are toxic to the cells. In such cases, culture growth is inhibited. To manage the toxicity, they resorted to using the inducible nitrate assimilation *NIR* promoter of the filamentous cyanobacterium *Anabaena*, as the promoter of their transgenes. The latter is repressed in the presence of ammonium ( $NH_4^+$ ) salts but induced in the absence of ammonium and the presence of nitrate ( $NO_3^-$ ). They promoted *Anabaena* growth to high cell density in the presence of ammonium ( $NH_4^+$ ), thereby blocking the expression of the transgenes. When ammonium was replaced with nitrate salts, cells then activated the *NIR* promoter, as they were forced to rely on nitrate nutrients for further growth. This induction process, entailing terminal cell growth and product generation, offered some success in overcoming product toxicity but cannot be easily applied to scale.

Results in this work showed a third level of difficulty in the attempt to overexpress eukaryotic recombinant proteins in photosynthetic microorganisms, that of product instability in the host cell. The latter is evidenced by the fact that diverse eukaryotic recombinant proteins, exemplified by the kudzu isoprene synthase and the human  $\alpha$ -interferon, can be overexpressed to 10–20% of the total cellular protein as fusion constructs. However, when cleaved from their stabilizing leader sequence and released in the cyanobacterial cytosol, they were efficiently degraded and either could not be detected or could be detected as residual faint protein bands (Figures 7 and 8).

Paradoxically, the above difficulties did not seem to apply to bacterial overexpression of a variety of prokaryotic recombinant proteins.<sup>21,33,43</sup> In this context, the tetanus toxin fragment C protein was overexpressed in this work, as a fusion construct with the *cpcB* gene, to about 20% of the total cellular protein. Importantly, when cleaved from its leader sequence *in vivo* and released in the cyanobacterial cytosol, the free TTFC appeared to accumulate as a soluble protein even further, apparently untouched by the cellular proteolysis apparatus (Figures 9B and 9C). In the context of this work, and among the recombinant proteins examined, only the TTFC proved to be stable, whereas the other recombinant proteins (ISPS and IFN) were degraded by the cell (Figure 11).

These results exemplify how eukaryotic proteins ISPS and IFN are unstable in cyanobacteria and also point to the fact that this difficulty can be overcome by the fusion constructs approach employed in this work. They also corroborate the accumulating evidence that at least some recombinant bacterial proteins can be heterologously overexpressed in cyanobacteria by using strong endogenous or exogenous promoters, with or without the fusion constructs approach.<sup>10,21–24,27,44</sup>

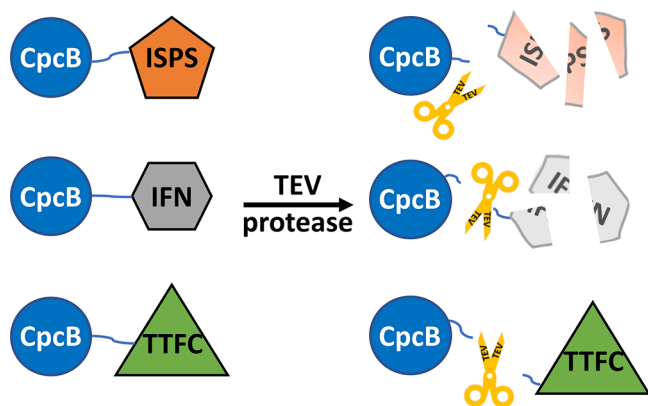


**Figure 11.** Schematic depicting the activity of TEV on the CpcB\*tev\*ISPS (upper), CpcB\*tev\*IFN (middle), and CpcB\*tev\*TTFC (lower) fusion protein constructs. In all cases, proteolytic cleavage of the “tev” domain by the TEV protease resulted in the separation and release of the ISPS, IFN, and TTFC from the CpcB fusion configuration, respectively. The schematic also depicts how the eukaryotic isoprene synthase (ISPS), a vascular plant protein, and interferon (IFN), a human protein, were unstable as free proteins and were degraded by the cyanobacterial cytosol. On the contrary, the prokaryotic tetanus toxin fragment C protein (TTFC) was stable upon cleavage of the “tev” domain and accumulated as a free protein to high levels in the cyanobacterial cells.

Further support for the apparent compatibility of prokaryotic protein expression in cyanobacteria is offered by the work of Zhou et al.,<sup>44</sup> who described the function of a modified (partial) endogenous cyanobacterial promoter (*Pcpc560*), derived from the native cyanobacterial *Pcpc* promoter, and examined the efficacy of this modified promoter to express (i) the trans-enoyl-CoA reductase (Ter) protein from *Treponema denticola*, a Gram-negative, obligate anaerobic bacterium, and (ii) the D-lactate dehydrogenase (DldhE) protein from *Escherichia coli*. Both of these bacterial-origin genes and recombinant proteins were overexpressed in cyanobacteria under the control of the *Pcpc* promoter, consistent with findings on the expression of other heterologous bacterial genes (see below). Similarly, the *nptI* gene from *Escherichia coli*, encoding a kanamycin resistance protein,<sup>21</sup> the *cmR* gene from *Escherichia coli*, encoding a chloramphenicol resistance protein,<sup>45</sup> and the isopentenyl diphosphate isomerase (*fni*) gene from *Streptococcus pneumoniae*,<sup>33</sup> all were easily and directly overexpressed in *Synechocystis* under the control of different promoters and as part of different transgenic DNA construct configurations.

It is of interest that a low level of TEV (Figure 2), when coexpressed along with the *cpcB\*L7\*L7\*tev\*ISPS*, *cpcB\*tev\*IFN*, and *cpcB\*tev\*TTFC* fusion constructs was necessary and sufficient to cleave and release recombinant proteins (ISPS, IFN, or TTFC) from their fusion construct configuration (Figures 7, 8 and 9). However, the low expression level of the TEV, in spite of concerted efforts in the course of this work to overexpress it, may suggest that viral proteins are also unstable in cyanobacteria, even under the control of strong promoters such as those of the *psbA2* and *P<sub>TRC</sub>*.

## METHODS

**Strains, Recombinant Constructs, and Culture Conditions.** The cyanobacterium *Synechocystis* sp. PCC 6803

(*Synechocystis*) was used as the experimental strain in this work and referred to as the wild type (WT). Gene sequences encoding the tetanus toxin fragment C (Genbank AF154828.1), SUMO (ENA EDN60828, depleted of the three 3' codons encoding the C-terminus residues ATY), and TEV protease (<https://qb3.berkeley.edu/facility/qb3-macro-lab/#:~:text=Your%20TEV%20Protease&text=Your%20box%20of%20TEV%20contains,subtractive%20nickel%20column%20with%20it>, without the N-terminal His-tag) were codon optimized for protein expression in *Synechocystis* using the IDT open software (<https://www.idtdna.com/CodonOpt>). DNA constructs for *Synechocystis* transformation were synthesized at Biomatik USA (Wilmington, DE). Constructs for expressing the kudzu isoprene synthase (ISPS) and the  $\alpha$ -interferon in *Synechocystis* were available in the lab from previous experimental work.<sup>20,25</sup> Generation of mutations, insertions, or deletions in plasmid DNA constructs were conducted via the Q5 Site-Directed Mutagenesis Kit (New England Biolabs, Ipswich, MA). Sequences of the various DNA constructs are shown in the Supporting Information.

*Synechocystis* transformations were carried out according to established protocols.<sup>36,46,47</sup> Wild type and transformants were maintained on BG11 media supplemented with 1% agar, 10 mM TES-NaOH (pH 8.2), and 0.3% sodium thiosulfate. Liquid cultures of BG11 were buffered with 25 mM sodium bicarbonate and 25 mM dipotassium hydrogen phosphate and incubated in the light upon slow continuous bubbling with air at 26 °C. Transgenic DNA copy homoplasmy in the cells was achieved upon transformant incubation on agar in the presence of increasing concentrations of the proper antibiotic (chloramphenicol, kanamycin spectinomycin, 3–25  $\mu\text{g}/\text{mL}$ ). Growth of the cells was promoted by using a balanced combination of white LED bulbs supplemented with incandescent light to yield a final photosynthetically active radiation (PAR) intensity of  $\sim 100 \mu\text{mol photons m}^{-2} \text{ s}^{-1}$ .

**Genomic DNA PCR Analysis of *Synechocystis* Transformants.** Genomic DNA templates were prepared, as previously described.<sup>14</sup> A 20  $\mu\text{L}$  culture aliquot was provided with an equal volume of 100% ethanol followed by brief vortexing. A 200  $\mu\text{L}$  aliquot of a 10% (w/v) Chelex100 Resin (BioRad, Hercules, CA) suspension in water was added to the sample prior to mixing and heating at 98 °C for 10 min to lyse the cells. Following centrifugation at 16,000g for 10 min to pellet cell debris, 5  $\mu\text{L}$  of the supernatant was used as a genomic DNA template in a 25  $\mu\text{L}$  PCR reaction mixture. Q5 DNA polymerase (New England Biolabs, Ipswich, MA) was used to perform the genomic DNA PCR analyses. Transgenic DNA copy homoplasmy in *Synechocystis* was tested using suitable primers listed in the Supporting Information Table S1. The genomic DNA location of these primers is indicated in the figures with forward and reverse arrows for the appropriate DNA constructs.

**Protein Analysis.** Cells in the mid-exponential growth phase ( $\text{OD}_{730} = \sim 1$ ) were harvested by centrifugation at 4,000g for 10 min. The pellet was resuspended in a solution buffered with 25 mM Tris-HCl, pH 8.2, also containing a cComplete mini protease inhibitor cocktail (Roche; one 50 mg tablet was added per 50 mL suspension). Cells were broken by passing the suspension through a French press cell at 1,500 psi. A slow speed centrifugation (350 g for 3 min) was applied to remove unbroken cells and sizable cell debris. For protein electrophoretic analysis, cell extracts were solubilized upon incubation for 20 min at 42 °C in the presence of 1x Laemmli

Sample Buffer (BioRad, Hercules, CA), supplemented with both 2 M urea and 5%  $\beta$ -mercaptoethanol. During the 20 min incubation, samples were vortexed every 10 min for 10 s. SDS-PAGE was performed using Mini-PROTEAN TGX precast gels (BioRad, Hercules, CA). Densitometric quantification of target proteins, as a percentage of the total cellular protein, was performed using the BioRad (Hercules, CA) Image Lab software. A subsequent Western blot analysis entailed transfer of the SDS-PAGE-resolved proteins to a 0.2  $\mu$ m pore size PVDF membrane (Life Technologies, Carlsbad, CA). Protein transfer to PVDF, conducted overnight at constant 20 V and 4  $^{\circ}$ C, was followed by protein probing with rabbit-raised CpcB- (PhytoAB, Redwood City, CA), TEV- (BioVision, Milpitas, CA), TTFC- (Antibodies-Online, Limerick, PA), ISPS-,<sup>25,36</sup> or IFN-specific polyclonal antibodies.<sup>20</sup>

**Isoprene and Biomass Accumulation.** Liquid cultures for isoprene production were grown photoautotrophically. Glass bottle bioreactors (1 L volume) designed in this lab<sup>48</sup> were loaded with  $\sim$ 550 mL liquid BG11 growth medium, buffered with  $K_2HPO_4$  and  $NaHCO_3$ , and then inoculated with *Synechocystis* starter cultures to an OD<sub>730 nm</sub> = 0.65. Unless otherwise indicated, the bioreactors were further loaded with inorganic carbon, delivered to the liquid culture by slowly bubbling 500 mL of 100% CO<sub>2</sub> gas through the bottom of the liquid culture to fill the reactor headspace. Bioreactors were then sealed and cultures were stirred slowly and continuously at 28  $^{\circ}$ C under constant illumination at around 100  $\mu$ mol photons m<sup>-2</sup> s<sup>-1</sup>.

Isoprene accumulation in the headspace of the reactor was determined by gas chromatography (Shimadzu 8A GC-FID) analysis of 1 mL gaseous samples from the bioreactor headspace. Isoprene quantification was determined based on a calibration of the isoprene standard (Acros Organics, Fair Lawn, NJ, USA), as described. Biomass accumulation in the liquid phase of the reactor was determined upon collection of 50 mL aliquots, followed by centrifugation and cell resuspension in 2 mL of deionized water. The latter were transferred onto aluminum trays, dried overnight at 60  $^{\circ}$ C, and weighed to determine the dry cell weight (dcw).

**Data Availability Statement.** All data sets generated and analyzed in this work are included in the manuscript's Supporting Information. Moreover, the codon-optimized nucleotide sequences, as expressed in *Synechocystis* for the purposes of this work, and the nucleotide sequences of the full constructs that were synthesized and employed are also shown in the Supporting Information.

**Statistical Analysis of the Results.** Measurements were conducted in triplicate with essentially the same results, although a single representative figure from each experiment is shown.

## ■ ASSOCIATED CONTENT

### SI Supporting Information

The Supporting Information is available free of charge at <https://pubs.acs.org/doi/10.1021/acssynbio.0c00610>.

Supplemental tables: Table S1, sequence of oligonucleotide primers used in the present work; Table S2, quantification of the heterologous Tetanus Toxin Fragment C (TTFC) protein in various TTFC transformants of *Synechocystis*. Supplemental figures: Figure S1, absorbance spectra of *Synechocystis* wild type and the various fusion construct transformants; Figure S2,

isoprene accumulation in the transformants of *Synechocystis*; sequence of the DNA constructs employed for the transformation of *Synechocystis*. Supplemental construct maps and DNA sequences: *nptI-TEV*; *nptI\*TEV*; *SUMO\*TEV-nptI*; *cpcB\*L7\*tev\*ISPS-cmR*; *cpcB\*L7\*L7\*tev\*ISPS-cmR*; *cpcB\*L7\*(GGGS)<sub>2</sub>\*tev\*ISPS-cmR*; *cpcB\*tev\*IFN-cmR*; *cpcB\*tev\*TTFC-smR*;  $\Delta$ *cpc-TTFC-smR*. (PDF)

## ■ AUTHOR INFORMATION

### Corresponding Author

Anastasios Melis – Department of Plant and Microbial Biology, University of California, Berkeley, California 94720-3102, United States; [orcid.org/0000-0003-2581-4177](https://orcid.org/0000-0003-2581-4177); Email: [melis@berkeley.edu](mailto:melis@berkeley.edu)

### Authors

Xianan Zhang – Department of Plant and Microbial Biology, University of California, Berkeley, California 94720-3102, United States

Nico Betterle – Department of Plant and Microbial Biology, University of California, Berkeley, California 94720-3102, United States; [orcid.org/0000-0002-7556-6696](https://orcid.org/0000-0002-7556-6696)

Diego Hidalgo Martinez – Department of Plant and Microbial Biology, University of California, Berkeley, California 94720-3102, United States

Complete contact information is available at:

<https://pubs.acs.org/10.1021/acssynbio.0c00610>

### Author Contributions

<sup>†</sup>X.Z., N.B., and D.H.M. contributed equally to this work.

### Funding

This work was supported by UC Berkeley Fund 45033. Xianan Zhang acknowledges financial support from the China Scholarship Council (CSC), Grant No. 201908110037, during her visit and work at Berkeley.

### Notes

The authors declare no competing financial interest.

## ■ ABBREVIATIONS

TEV, tobacco etch virus protease; *tev*, tobacco etch virus protease cleavage site; *nptI-TEV*,  $P_{TRC}$ -*nptI-TEV-PsbA2T*; *nptI\*TEV*,  $P_{TRC}$ -*nptI\*(GGGS)<sub>2</sub>\*TEV-PsbA2T*; *SUMO\*TEV*,  $P_{TRC}$ -*SUMO\*TEV-KanR-PsbA2T*; R (recipient), *cpcB\*L7\*ISPS-cmR+cpc*; *\*tev*, *cpcB\*L7\*tev\*ISPS-cmR+cpc*; *L\*tev*, *cpcB\*L7\*L7\*tev\*ISPS-cmR+cpc*; *G\*tev*, *cpcB\*L7\*(GGGS)<sub>2</sub>\*tev\*ISPS-cmR+cpc*; *L\*tev+nptI\*TEV*, double *L\*tev* and *nptI\*TEV* transformant; *L\*tev+SUMO\*TEV*, double *L\*tev* and *SUMO\*TEV* transformant; *L\*tev+nptI-TEV*, double *L\*tev* and *nptI-TEV* transformant

## ■ REFERENCES

- (1) Pulz, O., and Gross, W. (2004) Valuable products from biotechnology of microalgae. *Appl. Microbiol. Biotechnol.* 65, 635–648.
- (2) Ducat, D. C., Way, J. C., and Silver, P. A. (2011) Engineering cyanobacteria to generate high-value products. *Trends Biotechnol.* 29, 95–103.
- (3) Scranton, M. A., Ostrand, J. T., Fields, F. J., and Mayfield, S. P. (2015) Chlamydomonas as a model for biofuels and bio-products production. *Plant J.* 82, 523–531.
- (4) Goma, M. A., Al-Haj, L., and Abed, R. M. M. (2016) Metabolic engineering of Cyanobacteria and microalgae for enhanced

- production of biofuels and high-value products. *J. Appl. Microbiol.* 121, 919–931.
- (5) Knoot, C. J., Ungerer, J., Wangikar, P. P., and Pakrasi, H. B. (2018) Cyanobacteria: Promising biocatalysts for sustainable chemical production. *J. Biol. Chem.* 293, 5044–5052.
- (6) Khan, S., and Fu, P. (2020) Biotechnological perspectives on algae: a viable option for next generation biofuels. *Curr. Opin. Biotechnol.* 62, 146–152.
- (7) García, J. L., de Vicente, M., and Galán, B. (2017) Microalgae, old sustainable food and fashion nutraceuticals. *Microb. Biotechnol.* 10, 1017–1024.
- (8) Skjånes, K., Rebours, C., and Lindblad, P. (2013) Potential for green microalgae to produce hydrogen, pharmaceuticals and other high value products in a combined process. *Crit. Rev. Biotechnol.* 33, 172–215.
- (9) Angermayr, S. A., Gorchs Rovira, A., and Hellingwerf, K. J. (2015) Metabolic engineering of cyanobacteria for the synthesis of commodity products. *Trends Biotechnol.* 33, 352–361.
- (10) Vijay, D., Akhtar, M. K., and Hess, W. R. (2019) Genetic and metabolic advances in the engineering of cyanobacteria. *Curr. Opin. Biotechnol.* 59, 150–156.
- (11) Yu, J., Liberton, M., Cliften, P. F., Head, R. D., Jacobs, J. M., Smith, R. D., Koppenaal, D. W., Brand, J. J., and Pakrasi, H. B. (2015) *Synechococcus elongatus* UTEX 2973, a fast growing cyanobacterial chassis for biosynthesis using light and CO<sub>2</sub>. *Sci. Rep.* 5, 8132.
- (12) Jaiswal, D., Sengupta, A., Sohoni, S., Sengupta, S., Phadnavis, A. G., Pakrasi, H. B., and Wangikar, P. P. (2018) Genome Features and Biochemical Characteristics of a Robust, Fast Growing and Naturally Transformable Cyanobacterium *Synechococcus elongatus* PCC 11801 Isolated from India. *Sci. Rep.* 8, 16632.
- (13) Włodarczyk, A., Selão, T. T., Norling, B., and Nixon, P. J. (2020) Newly discovered *Synechococcus* sp. PCC 11901 is a robust cyanobacterial strain for high biomass production. *Commun. Biol.* 3, 215.
- (14) Formighieri, C., and Melis, A. (2014) Regulation of  $\beta$ -phellandrene synthase gene expression, recombinant protein accumulation, and monoterpene hydrocarbons production in *Synechocystis* transformants. *Planta* 240, 309–324.
- (15) Thiel, K., Mulaku, E., Dandapani, H., Nagy, C., Aro, E. M., and Kallio, P. (2018) Translation efficiency of heterologous proteins is significantly affected by the genetic context of RBS sequences in engineered cyanobacterium *Synechocystis* sp. PCC 6803. *Microb. Cell Fact.* 17, 1–12.
- (16) Wang, B., Eckert, C., Maness, P.-C., and Yu, J. (2018) A Genetic Toolbox for Modulating the Expression of Heterologous Genes in the Cyanobacterium *Synechocystis* sp. PCC 6803. *ACS Synth. Biol.* 7, 276–286.
- (17) Gordon, G. C., and Pflieger, B. F. (2018) Regulatory Tools for Controlling Gene Expression in Cyanobacteria. *Adv. Exp. Med. Biol.* 1080, 281–315.
- (18) Santos-Merino, M., Singh, A. K., and Ducat, D. C. (2019) New Applications of Synthetic Biology Tools for Cyanobacterial Metabolic Engineering. *Front. Bioeng. Biotechnol.* 7, 33.
- (19) Du, W., Jongbloets, J. A., Guillaume, M., van de Putte, B., Battagliano, B., Hellingwerf, K. J., and Branco Dos Santos, F. (2019) Exploiting Day- and Night-Time Metabolism of *Synechocystis* sp. PCC 6803 for Fitness-Coupled Fumarate Production around the Clock. *ACS Synth. Biol.* 8, 2263–2269.
- (20) Betterle, N., Hidalgo Martinez, D., and Melis, A. (2020) Cyanobacterial Production of Biopharmaceutical and Biotherapeutic Proteins. *Front. Plant Sci.* 11, 1–16.
- (21) Kirst, H., Formighieri, C., and Melis, A. (2014) Maximizing photosynthetic efficiency and culture productivity in cyanobacteria upon minimizing the phycobilisome light-harvesting antenna size. *Biochim. Biophys. Acta, Bioenerg.* 1837, 1653–1664.
- (22) Formighieri, C., and Melis, A. (2015) A phycocyanin<sup>+</sup>phellandrene synthase fusion enhances recombinant protein expression and  $\beta$ -phellandrene (monoterpene) hydrocarbons production in *Synechocystis* (cyanobacteria). *Metab. Eng.* 32, 116–124.
- (23) Xiong, W., Morgan, J. A., Ungerer, J., Wang, B., Maness, P.-C., and Yu, J. (2015) The plasticity of cyanobacterial metabolism supports direct CO<sub>2</sub> conversion to ethylene. *Nat. Plants* 1, 15053.
- (24) Formighieri, C., and Melis, A. (2016) Sustainable heterologous production of terpene hydrocarbons in cyanobacteria. *Photosynth. Res.* 130, 123–135.
- (25) Chaves, J. E., Rueda-romero, P., Kirst, H., and Melis, A. (2017) Engineering Isoprene Synthase Expression and Activity in Cyanobacteria. *ACS Synth. Biol.* 6, 2281–2292.
- (26) Choi, S. Y., Wang, J.-Y., Kwak, H. S., Lee, S.-M., Um, Y., Kim, Y., Sim, S. J., Choi, J.-I., and Woo, H. M. (2017) Improvement of Squalene Production from CO<sub>2</sub> in *Synechococcus elongatus* PCC 7942 by Metabolic Engineering and Scalable Production in a Photobioreactor. *ACS Synth. Biol.* 6, 1289–1295.
- (27) Betterle, N., and Melis, A. (2018) Heterologous Leader Sequences in Fusion Constructs Enhance Expression of Geranyl Diphosphate Synthase and Yield of  $\beta$ -Phellandrene Production in Cyanobacteria (*Synechocystis*). *ACS Synth. Biol.* 7, 912–921.
- (28) Betterle, N., and Melis, A. (2019) Photosynthetic generation of heterologous terpenoids in cyanobacteria. *Biotechnol. Bioeng.* 116, 2041–2051.
- (29) Valsami, E.-A., Psychogyiou, M. E., Pateraki, A., Chrysoulaki, E., Melis, A., and Ghanotakis, D. F. (2020) Fusion constructs enhance heterologous  $\beta$ -phellandrene production in *Synechocystis* sp. PCC 6803. *J. Appl. Phycol.* 32, 2889–2902.
- (30) Lauersen, K. J., Wichmann, J., Baier, T., Kampranis, S. C., Pateraki, I., Møller, B. L., and Kruse, O. (2018) Phototrophic production of heterologous diterpenoids and a hydroxy-functionalized derivative from *Chlamydomonas reinhardtii*. *Metab. Eng.* 49, 116–127.
- (31) Shih, Y.-P., Wu, H.-C., Hu, S.-M., Wang, T.-F., and Wang, A. H.-J. (2005) Self-cleavage of fusion protein in vivo using TEV protease to yield native protein. *Protein Sci.* 14, 936–941.
- (32) Muto, M., Henry, R. E., and Mayfield, S. P. (2009) Accumulation and processing of a recombinant protein designed as a cleavable fusion to the endogenous Rubisco LSU protein in *Chlamydomonas chloroplast*. *BMC Biotechnol.* 9, 1–11.
- (33) Chaves, J. E., and Melis, A. (2018) Biotechnology of cyanobacterial isoprene production. *Appl. Microbiol. Biotechnol.* 102, 6451–6458.
- (34) Peroutka, R. J., III, Orcutt, S. J., Strickler, J. E., and Butt, T. R. (2011) SUMO Fusion Technology for Enhanced Protein Expression and Purification in Prokaryotes and Eukaryotes, in *Heterologous Gene Expression in E. coli: Methods and Protocols* (Evans, T. C., Jr., and Xu, M.-Q., Eds.), pp 15–30, Humana Press, Totowa, NJ.
- (35) Robinson, K., Chamberlain, L. M., Schofield, K. M., Wells, J. M., and Le Page, R. W. F. (1997) Oral vaccination of mice against tetanus with recombinant *Lactococcus lactis*. *Nat. Biotechnol.* 15, 653–657.
- (36) Lindberg, P., Park, S., and Melis, A. (2010) Engineering a platform for photosynthetic isoprene production in cyanobacteria, using *Synechocystis* as the model organism. *Metab. Eng.* 12, 70–79.
- (37) Bentley, F. K., García-Cerdán, J. G., Chen, H.-C., and Melis, A. (2013) Paradigm of Monoterpene ( $\beta$ -phellandrene) Hydrocarbons Production via Photosynthesis in Cyanobacteria. *BioEnergy Res.* 6, 917–929.
- (38) Formighieri, C., and Melis, A. (2017) Heterologous synthesis of geranylinalool, a diterpenol plant product, in the cyanobacterium *Synechocystis*. *Appl. Microbiol. Biotechnol.* 101 (7), 2791–2800.
- (39) Rasala, B. A., Muto, M., Lee, P. A., Jager, M., Cardoso, R. M. F., Behnke, C. A., Kirk, P., Hokanson, C. A., Crea, R., Mendez, M., and Mayfield, S. P. (2010) Production of therapeutic proteins in algae, analysis of expression of seven human proteins in the chloroplast of *Chlamydomonas reinhardtii*. *Plant Biotechnol. J.* 8, 719–733.
- (40) Coragliotti, A. T., Beligni, M. V., Franklin, S. E., and Mayfield, S. P. (2011) Molecular factors affecting the accumulation of recombinant proteins in the *Chlamydomonas reinhardtii* chloroplast. *Mol. Biotechnol.* 48, 60–75.

- (41) Qin, D., and Fredrick, K. (2013) Analysis of polysomes from bacteria. *Methods Enzymol.* 530, 159–172.
- (42) Desplancq, D., Rinaldi, A.-S., Hörzer, H., Ho, Y., Nierengarten, H., Atkinson, R. A., Kieffer, B., and Weiss, E. (2008) Automated overexpression and isotopic labelling of biologically active oncoproteins in the cyanobacterium *Anabaena* sp. PCC 7120. *Biotechnol. Appl. Biochem.* 51, 53–61.
- (43) Lim, H., Park, J., and Woo, H. M. (2020) Overexpression of the Key Enzymes in the Methylerythritol 4-phosphate Pathway in *Corynebacterium glutamicum* for Improving Farnesyl Diphosphate-Derived Terpene Production. *J. Agric. Food Chem.* 68, 10780–10786.
- (44) Zhou, J., Zhang, H., Meng, H., Zhu, Y., Bao, G., Zhang, Y., Li, Y., and Ma, Y. (2014) Discovery of a super-strong promoter enables efficient production of heterologous proteins in cyanobacteria. *Sci. Rep.* 4, 1–6.
- (45) Chaves, J. E., Romero, P. R., Kirst, H., and Melis, A. (2016) Role of isopentenyl-diphosphate isomerase in heterologous cyanobacterial (*Synechocystis*) isoprene production. *Photosynth. Res.* 130, 517–527.
- (46) Williams, J. G. K. (1988) Construction of Specific Mutations in Photosystem II Photosynthetic Reaction Center by Genetic Engineering Methods in *Synechocystis* 6803. *Methods Enzymol.* 167, 766–778.
- (47) Eaton-Rye, J. J. (2011) Construction of Gene Interruptions and Gene Deletions in the Cyanobacterium *Synechocystis* sp. Strain PCC 6803. In *Photosynthesis Research Protocols. Methods in Molecular Biology (Methods and Protocols)* Carpentier, R., Eds.), Vol 684, Humana Press, Totowa.
- (48) Bentley, F. K., and Melis, A. (2012) Diffusion-based process for carbon dioxide uptake and isoprene emission in gaseous/aqueous two-phase photobioreactors by photosynthetic microorganisms. *Biotechnol. Bioeng.* 109, 100–109.